MATHEMATICAL BIOSCIENCES
AND ENGINEERING
Volume **13**, Number **2**, April **2016**

doi:10.3934/mbe.2015006
pp. **343–367**

# BIFURCATION ANALYSIS OF HIV-1 INFECTION MODEL WITH CELL-TO-CELL TRANSMISSION AND IMMUNE RESPONSE DELAY

Jinhu Xu and Yicang Zhou*

School of Mathematics and Statistics
Xi'an Jiaotong University
Xi'an, 710049, China

(Communicated by Jia Li)

Abstract. A within-host viral infection model with both virus-to-cell and cell-to-cell transmissions and time delay in immune response is investigated. Mathematical analysis shows that delay may destabilize the infected steady state and lead to Hopf bifurcation. Moreover, the direction of the Hopf bifurcation and the stability of the periodic solutions are investigated by normal form and center manifold theory. Numerical simulations are done to explore the rich dynamics, including stability switches, Hopf bifurcations, and chaotic oscillations.

1. **Introduction.** Human Immunodeficiency Virus (HIV) and Acquired Immune Deficiency Syndrome (AIDS) have spread in successive waves in various regions and kept being a serious threat to public health. HIV targets cells with CD4 receptors, including the $CD4^+$ T-cells, and damages the body's immune system, leading to humoral and cellular immune function loss (the marker of the onset of AIDS), making the body susceptible to opportunistic infections. The earlier models of virus infection describe the interaction between virus and target cells by assuming that the infected cells produce virions instantaneously [1, 2].

The early models of virus infections, given by ordinary differential equations (ODEs), ignore the time delays of the viral infection, production of subsequent virus particles, and activation of immune response. Ciupe et al. [3] have shown that allowing for time delays in the model better predicts viral load data when compared to models without delays. The introduction of delays make the models more realistic. A discrete delay was first introduced into HIV infection model by Herz et al. [4]. Various models of viral dynamics with discrete or distributed delays have generally been studied [5–16].

We noticed that most within-host virus models concentrate on the virus-to-cell transmission. In fact, the infection via cell-to-cell contact is found to be much more rapid and efficient than virus-to-cell transmission because it avoids several

2010 *Mathematics Subject Classification.* Primary: 34K20, 92D30; Secondary: 34C23, 34K60.
*Key words and phrases.* Cell-to-cell transmission, time delay, Hopf bifurcation, stability switches, chaotic oscillations.
This work was supported by the National Natural Science Foundation of China (#11301314, #11501443), and by a grant (# 104519-010) from the International Development Research Center, Ottawa, Canada.
* Corresponding author: Yicang Zhou, zhouyc@mail.xjtu.edu.cn.

biophysical and kinetic barriers [17]. It has been reported that cell-to-cell spread of virus is favored over infections with cell-free virus inocula [18, 19]. The data of Gummuluru et al. [20] support the hypothesis that cell-to-cell spread of HIV-1 is the predominant route of viral spread since viral replication in a system with rapid cell turnover kinetics depends on cell-to-cell transfer of virus. Cell-to-cell transmission has also been reported for many other infections, such as HCV [21–23], Epstein Barr Virus (EBV) [24], Herpes simplex virus type-1 (HSV-1) [25], and HTLV-1 [26]. The mechanisms cell-to-cell transmission mode were, however, not well understood until the recent description of the "virological synapses" (VSs) [27]. Cell-to-cell spread greatly influences pathogenesis, not only facilitates rapid viral dissemination but may also promote immune invasion and, thereby, influence the disease [28–30]. As far as cell-to-cell infection is concerned, much less has been done in mathematical modeling. Culshaw et al. [11] studied a delayed two-dimensional model of cell-to-cell spread of HIV-1 in tissue cultures with logistic growth term for target cells, assuming that infection is spread directly from infected cells to healthy cells and neglecting the effects of free virus. Thereafter, Lai and Zou [31] studied a virus model with both virus-to-cell infection and cell-to-cell infection. These authors also considered a model which including both cell-to-cell infection and full logistic growth term for target cells [32],

$$\begin{cases} \frac{dT}{dt} = rT(t)\left(1 - \frac{T(t)+\alpha I(t)}{T_{max}}\right) - \beta_1 T(t)V(t) - \beta_2 T(t)I(t), \\ \frac{dI}{dt} = \beta_1 T(t)V(t) + \beta_2 T(t)I(t) - d_1 I(t), \\ \frac{dV}{dt} = \gamma I(t) - d_2 V(t). \end{cases} \tag{1}$$

Here $T(t), I(t)$ and $V(t)$ represent the concentrations of susceptible $CD4^+$ T cells (target cells), productively infected T cells and free virus particles at time $t$, respectively. Target cells are infected by free viral particles and infectious cells (productively infected cells) at rates $\beta_1 T(t)V(t)$ and $\beta_2 T(t)I(t)$, respectively. $r, T_{max}, \gamma, d_1$ and $d_2$ represent the growth rate of a target cell, carrying capacity of target cells, the rate of free viral particles released by infected cells, the losing rate of productively infected cells and free viruses, respectively. $\alpha$ ($\alpha \geq 1$) is the limitation coefficient of infected cells imposed on the growth of target cells. The stability, persistence as well as Hopf bifurcation of model (1) have been investigated.

The immune response has not been considered in model (1) though antibodies, cytokines, natural killer cells, and T cells are essential components of a normal immune response to a virus. In most virus infections, cytotoxic T lymphocytes (CTLs) play a critical role in antiviral defense by attacking virus-infected cells. Indeed, in HIV infection, CTLs are the main host factors which determine viral load. The dynamics of HIV infection with CTL response has received much attention in the past decades [3, 5, 12, 13, 16, 33, 34]. For example, Ciupe et al. [3] considered the following delayed HIV model

$$\begin{cases} \frac{dT}{dt} = rT(t)\left(1 - \frac{T(t)+I(t)}{T_{max}}\right) - kT(t)V(t), \\ \frac{dI}{dt} = kT(t)V(t) - d_1 I(t) - d_3 E(t)I(t), \\ \frac{dV}{dt} = Nd_1 I(t) - d_2 V(t), \\ \frac{dE}{dt} = pI(t-\tau) - d_4 E(t). \end{cases} \tag{2}$$

Here $E(t)$ is the concentration of effector cells. The constant $r$ is the growth rate of target cells and the growth is limited by a carrying capacity $T_{max}$. Target cells

are infected by free viral particles at rates $kT(t)V(t)$. $d_1$, $d_3$, $N$, $d_2$, $p$ and $d_4$ represent the death rate of productive infected cells, the killing rate of infected cells by effector cells, the number of virions produced by an infected cell during its life span (burst size), the viral clearance rate and productive rate of the effector cells and the death rate of effector cells, respectively. The term $I(t-\tau)$ accounts for the time needed to activate the $CD8^+$ T cell response, where $\tau$ is a constant. The authors mainly focused on estimating the kinetic parameters of model (2) while the dynamics behavior of model (2) has not been studied. The cell-to-cell transmission has not been taken into consideration in model (2).

Motivated by [3, 32], we consider the following model

$$\begin{cases} \frac{dT}{dt} = s - dT(t) + rT(t)\left(1 - \frac{T(t)+\alpha I(t)}{T_{max}}\right) - \beta_1 T(t)V(t) - \beta_2 T(t)I(t), \\ \frac{dI}{dt} = \beta_1 T(t)V(t) + \beta_2 T(t)I(t) - d_1 I(t) - d_3 E(t)I(t), \\ \frac{dV}{dt} = N d_1 I(t) - d_2 V(t), \\ \frac{dE}{dt} = pI(t-\tau) - d_4 E(t), \end{cases} \tag{3}$$

with initial conditions

$$T(\theta) = \varphi_1(\theta),\ I(\theta) = \varphi_2(\theta),\ V(\theta) = \varphi_3(\theta),\ E(\theta) = \varphi_4(\theta),\ \theta \in [-\tau, 0], \tag{4}$$

where $\varphi = (\varphi_1, \varphi_2, \varphi_3, \varphi_4) \in C([-\tau, 0], \mathbb{R}^4_+)$ with $\varphi_i(\theta) > 0$ ($\theta \in [-\tau, 0]$, i=1,2,3,4) and $\varphi_2(0), \varphi_3(0), \varphi_4(0) > 0$. The constant $s$ is the source of $CD4^+$ T-cells from precursors, $d$ is the natural death rate ($d < r$ in general). The other parameters in model (3) have the same meaning with model (1) and (2).

The paper is organized as follows. In Section 2, we present some preliminaries. In Section 3, the dynamics behavior of infection-free steady state of model (3) is studied. Both the local stability of the infection steady state for model (3) and the conditions for the existence of Hopf bifurcation are presented. Furthermore, the properties of the Hopf bifurcation solutions have been investigated by applying normal form and center manifold theory. In Section 4, numerical simulations are carried out to show the rich and complex dynamics of model (3), such as Hopf bifurcation, stability switches phenomena and chaotic oscillations. Finally, a brief summary and discussions complete the paper.

## 2. **Preliminaries.**

We denote by $X = C([-\tau, 0], \mathbb{R}^4_+)$ the Banach space of continuous functions mapping the interval $[-\tau, 0]$ into $\mathbb{R}^4_+$ equipped with the sup-norm. By the standard theory of functional differential equations [35] we know that for any $\varphi \in C([-\tau, 0], \mathbb{R}^4_+)$ there exists a unique solution

$$\mathbf{Y}(t, \varphi) = (T(t, \varphi), I(t, \varphi), V(t, \varphi), E(t, \varphi))$$

of model (3) with initial condition (4).

**Theorem 2.1.** *Let $\mathbf{Y}(t, \varphi) = \{T(t), I(t), V(t), E(t)\}$ be the solution of model (3) with initial condition (4). Then $T(t), I(t), V(t), E(t)$ are positive for all $t \geq 0$, and they are ultimately bounded. Moreover, there exists an $\eta_0 > 0$ such that $\liminf_{t\to\infty} T(t) \geq \eta_0$.*

*Proof.* At first, we prove that $T(t)$ is positive for $t \geq 0$. Otherwise, there exists a positive $t_0$, such that $T(t) > 0$ for $t \in [0, t_0)$ and $T(t_0) = 0$. By the first equation of model (3), we have $T'(t_0) = s > 0$. $T'(t_0) = s > 0$ implies that $T(t) < 0$ for

$t \in (t_0 - \epsilon, t_0)$ and sufficiently small $\epsilon > 0$. This contradicts $T(t) > 0$ for $t \in [0, t_0)$. It follows that $T(t) > 0$ for $t > 0$. From the equation of (3) we have

$$\begin{aligned} I(t) =& I(0)e^{-\int_0^t (d_1 + d_3 E(\theta) - \beta_2 T(\theta))d\theta} + \int_0^t \beta_1 T(\theta) V(\theta) e^{-\int_\theta^t (d_1 + d_3 E(u) - \beta_2 T(u))du} d\theta, \\ V(t) =& V(0)e^{-d_2 t} + \int_0^t N d_1 I(\theta) e^{-d_2(t-\theta)} d\theta, \\ E(t) =& E(0)e^{-d_4 t} + \int_0^t p I(\theta - \tau) e^{-d_4(t-\theta)} d\theta. \end{aligned}$$

From those expressions and (4) we know that the solution of model (3) is positive for all $t \geq 0$.

Next, we show that the solution of model (3) is ultimately bounded. From the first equation of (3), we obtain

$$\frac{dT}{dt} \leq s - dT + rT\left(1 - \frac{T}{T_{max}}\right).$$

From this inequality and the comparison principle we know that $\limsup_{t\to\infty} T(t) \leq T_0$, where $T_0 = \frac{T_{max}}{2r}\left[r - d + \sqrt{(r-d)^2 + \frac{4rs}{T_{max}}}\right]$. Then $T(t)$ is ultimately bounded. Let $G = T(t) + I(t)$, then we have

$$\begin{aligned} G' \leq& s - dT + rT\left(1 - \frac{T}{T_{max}}\right) - d_1 I \\ \leq& s + rT\left(1 - \frac{T}{T_{max}}\right) - \delta(T + I) \\ \leq& K - \delta G, \end{aligned}$$

where $K = s + \frac{rT_{max}}{4}$ and $\delta = \min\{d, d_1\}$ . Thus, we have $\limsup_{t\to\infty} G \leq \frac{K}{\delta}$ and $I(t)$ is ultimately bounded. It follows from the third and fourth equations of (3),

$$V' \leq \frac{N d_1 K}{\delta} - d_2 V, \text{ and } E' \leq \frac{pK}{\delta} - d_4 E.$$

Therefore, we have $\limsup_{t\to\infty} V \leq \frac{N d_1 K}{d_2 \delta}$ and $\limsup_{t\to\infty} E \leq \frac{pK}{d_4 \delta}$. That is $V(t)$ and $E(t)$ are ultimately bounded. Furthermore, from the first equation of model (3) we have, for large $t$

$$T' \geq s - T\left(d - r + \frac{r(T_0 + \alpha\tilde{I})}{T_{max}} + \beta_1 \tilde{V} + \beta_2 \tilde{I}\right),$$

where $\tilde{I}$ and $\tilde{V}$ are the upper bounds of $I(t)$ and $V(t)$ respectively. This shows that $T(t)$ is uniformly bounded away from zero. □

Model (3) has two steady states: the infection-free steady state $P_0 = (T_0, 0, 0, 0)$, and the infected steady state $P_* = (T_*, I_*, V_*, E_*)$, where

$$\begin{aligned} T_0 =& \frac{T_{max}}{2r}\left[r - d + \sqrt{(r-d)^2 + \frac{4rs}{T_{max}}}\right], \\ T_* =& \frac{B + \sqrt{B^2 + 4As}}{2A}, \; I_* = \frac{d_4}{d_3 p}\left[\left(\beta_1 \frac{N d_1}{d_2} + \beta_2\right) T_* - d_1\right], \end{aligned}$$

$$
\begin{aligned}
V_* =& \frac{Nd_1}{d_2} I_*,\ E_* = \frac{pI_*}{d_4},\\
A =& \frac{r}{T_{max}} \frac{\alpha d_4}{d_3 p} \left( \frac{\beta_1 N d_1}{d_2} + \beta_2 \right) + \frac{d_4}{d_3 p} \left( \frac{\beta_1 N d_1}{d_2} + \beta_2 \right)^2,\\
B =& \frac{r}{T_{max}} \left( T_{max} + \frac{\alpha d_1 d_4}{d_3 p} \right) + \frac{d_1 d_4}{d_3 p} \left( \frac{\beta_1 N d_1}{d_2} + \beta_2 \right) - d.
\end{aligned}
$$

If we denote $R_0 = \dfrac{(\beta_1 N d_1 + \beta_2 d_2) T_0}{d_1 d_2}$, it is easy to validate that $R_0$ is the basic reproduction number of system (3). Biologically, $R_0$ represents the average number of secondary infections. In fact, the basic reproduction number $R_0$ includes two parts, we can rewrite $R_0$ as $R_0 = \beta_1 \cdot T_0 \cdot \frac{1}{d_1} \cdot N d_1 \cdot \frac{1}{d_2} + \beta_2 \cdot \frac{1}{d_1} \cdot T_0$. The first term is the average number of secondary infection caused by a virus, corresponding to virus-to-cell infection mode; the second term is the average number of secondary infection caused by an infected cell, corresponding to cell-to-cell infection. We can see that the basic reproduction number $R_0$ which we have defined is larger than that given in existing models with only one infection mode. The basic reproduction number of the model neglecting either the virus-to-cell infection or cell-to-cell infection may underevaluate the spread risk.

If $R_0 < 1$, then there is only the infection-free steady state. From the expression $I_*$, we know that the infected steady state exists if and only if $\left(\beta_1 \frac{N d_1}{d_2} + \beta_2\right) T_* > d_1$, which leads to $\left(\beta_1 \frac{N d_1}{d_2} + \beta_2\right) T_0 > d_1$, i.e. $R_0 > 1$. Vice versa, $R_0 \leq 1$ implies that $\left(\beta_1 \frac{N d_1}{d_2} + \beta_2\right) T_* < d_1$, thus there exists no infection steady state, i.e., only the infection-free steady state exists.

## 3. Dynamics analysis of model.

### 3.1. Stability of infection-free steady states $P_0$.

We linearize the model at steady states of model (3) to study the local stability. The characteristic equation is

$$
\begin{vmatrix}
\lambda + d + \beta_1 V + \beta_2 I + \frac{rT}{T_{max}} - r\left(1 - \frac{T+\alpha I}{T_{max}}\right) & \frac{\alpha r T}{T_{max}} + \beta_2 T & \beta_1 T & 0\\
-(\beta_1 V + \beta_2 I) & \lambda + d_1 + d_3 E - \beta_2 T & -\beta_1 T & d_3 I\\
0 & -N d_1 & \lambda + d_2 & 0\\
0 & -p e^{-\lambda \tau} & 0 & \lambda + d_4
\end{vmatrix} = 0.
$$

We have the following result for the infection-free steady state.

**Theorem 3.1.** *The infection-free steady state $P_0$ of model (3) is locally asymptotically stable when $R_0 < 1$ and unstable when $R_0 > 1$.*

*Proof.* At the infection-free steady state $P_0$, the characteristic equation becomes

$$
\left(\lambda + \frac{s}{T_0} + \frac{r T_0}{T_{max}}\right)(\lambda + d_4)[\lambda^2 + (d_2 + d_1 - \beta_2 T_0)\lambda + d_1 d_2 (1 - R_0)] = 0. \tag{5}
$$

There are two negative real roots: $\lambda_1 = -\left(\frac{s}{T_0} + \frac{r T_0}{T_{max}}\right)$, $\lambda_2 = -d_4$. The other roots satisfy

$$
\lambda^2 + (d_2 + d_1 - \beta_2 T_0)\lambda + d_1 d_2 (1 - R_0) = 0. \tag{6}
$$

The inequality $R_0 < 1$ implies that $d_2 + d_1 - \beta_2 T_0 > 0$, and all the roots of (6) have negative real part. Then the infection-free steady state $P_0$ is locally asymptotically stable. If $R_0 > 1$, then (6) has at least one root with positive real part. Thus, the infection-free steady state $P_0$ is unstable. □

**Theorem 3.2.** *The infection-free steady state $P_0$ of model (3) is globally asymptotically stable when $R_0 < 1$.*

*Proof.* For a continuous and bounded function $f(t)$, we define

$$f^\infty \triangleq \limsup_{t\to\infty} f(t) \text{ and } f_\infty \triangleq \liminf_{t\to\infty} f(t).$$

The solutions $T = T(t)$, $I = I(t)$, $V = V(t)$ and $E = E(t)$ of (3) satisfy

$$0 \le T_\infty \le T^\infty < \infty,\ 0 \le I_\infty \le I^\infty < \infty, \tag{7}$$

$$0 \le V_\infty \le V^\infty < \infty,\ 0 \le E_\infty \le E^\infty < \infty. \tag{8}$$

We claim that $T(t) \le T_0$ for $t \ge 0$ if $T(0) < T_0$. If there exists a $t_0 > 0$, such that $T(t) < T_0$ for $t \in [0, t_0)$, and $T(t_0) = T_0$, then $T'(t_0) > 0$. The first equation of model (3) implies that

$$\begin{aligned} T'(t_0) =& s - dT(t_0) + rT(t_0)\left(1 - \frac{T(t_0) + \alpha I(t_0)}{T_{max}}\right) - \beta_1 T(t_0)V(t_0) - \beta_2 T(t_0)I(t_0) \\ =& -\frac{\alpha r T_0 I(t_0)}{T_{max}} - \beta_1 T_0 V(t_0) - \beta_2 T_0 I(t_0) < 0, \end{aligned}$$

which contradicts $T'(t_0) > 0$.

From the fluctuation lemma [36], the second and third equations of model (3), we know that there is a sequence $t_n$ with $t_n \to \infty$ such that

$$d_1 I^\infty \le \beta_1 V^\infty T_0 + \beta_2 I^\infty T_0,\ d_2 V^\infty \le N d_1 I^\infty. \tag{9}$$

Those two inequalities lead to

$$d_1 I^\infty \le \left(\beta_1 \frac{N d_1}{d_2} + \beta_2\right) T_0 I^\infty. \tag{10}$$

$I^\infty$ is nonnegative since it is the supremum of the function $I(t)$. If $I^\infty > 0$, then the inequality in (10) yields

$$d_1 \le \left(\beta_1 \frac{N d_1}{d_2} + \beta_2\right) T_0,$$

which is contradiction with $R_0 < 1$. The possible case is $I^\infty = 0$, which implies $\lim_{t\to\infty} I(t) = 0$. From the inequality (9) and $I^\infty = 0$, we have $V^\infty = 0$, which implies that $\lim_{t\to\infty} V(t) = 0$. Similar argument to the fourth equation of system (3), we obtain $\lim_{t\to\infty} E(t) = 0$. By applying the limiting theory [37] to the first equation of system (3), we can obtain that $\lim_{t\to\infty} T(t) = T_0$. This completes the proof. □

3.2. **Stability of infected steady state $P_*$ and Hopf bifurcation.** In this section, we investigate the stability of the infected steady state and the existence of Hopf bifurcations. The infected steady state $P_*(T_*, I_*, V_*, E_*)$ satisfies

$$\begin{aligned} & s - dT_* + rT_*\left(1 - \frac{T_* + \alpha I_*}{T_{max}}\right) - \beta_1 T_* V_* - \beta_2 T_* I_* = 0, \\ & \beta_1 T_* V_* + \beta_2 T_* I_* = d_1 I_* + d_3 E_* I_*,\ V_* = \frac{N d_1}{d_2} I_*,\ E_* = \frac{p I_*}{d_4}. \end{aligned}$$

The characteristic equation at the infected steady state $P_*$ is

$$F(\lambda, \tau) = \lambda^4 + a_3\lambda^3 + a_2\lambda^2 + a_1\lambda + a_0 + (b_2\lambda^2 + b_1\lambda + b_0)e^{-\lambda\tau} = 0, \tag{11}$$

where $a_i > 0$ $(i = 0, 1, 2, 3)$, $b_i > 0$ $(i = 0, 1, 2)$, and

$$\begin{aligned}
a_3 =& \frac{r * T_*}{T_{max}} + \frac{s}{T_*} + d_2 + d_4 + \beta_1 \frac{N d_1}{d_2} T_*,\\
a_2 =& \left(\frac{r * T_*}{T_{max}} + \frac{s}{T_*}\right)\left(d_2 + d_4 + \beta_1 \frac{N d_1}{d_2} T_*\right) + d_4 \left(d_2 + \beta_1 \frac{N d_1}{d_2} T_*\right)\\
&+ \left(\beta_2 T_* + \frac{\alpha r T_*}{T_{max}}\right)\left(\beta_1 \frac{N d_1}{d_2} + \beta_2\right) I_*,\\
a_1 =& d_4 \left(d_2 + \beta_1 \frac{N d_1}{d_2} T_*\right)\left(\frac{r T_*}{T_{max}} + \frac{s}{T_*}\right) + \left(\beta_1 \frac{N d_1}{d_2} + \beta_2\right) I_* \Bigg[\beta_1 N d_1 T_*\\
&+ d_4 * \left(\beta_2 T_* + \frac{\alpha r T_*}{T_{max}}\right) + d_2 \left(\beta_2 T_* + \frac{\alpha r T_*}{T_{max}}\right)\Bigg],\\
a_0 =& d_4 \left(\beta_1 \frac{N d_1}{d_2} + \beta_2\right) I_* \left[\beta_1 N d_1 T_* + d_2 \left(\beta_2 T_* + \frac{\alpha r T_*}{T_{max}}\right)\right],\\
b_2 =& d_3 p I_*, \quad b_1 = d_3 p I_* \left(d_2 + \frac{r T_*}{T_{max}} + \frac{s}{T_*}\right), \quad b_0 = d_2 d_3 p I_* \left(\frac{r T_*}{T_{max}} + \frac{s}{T_*}\right).
\end{aligned}$$

When $\tau = 0$, the corresponding characteristic equation becomes

$$F(\lambda, 0) = \lambda^4 + a_3 \lambda^3 + (a_2 + b_2)\lambda^2 + (a_1 + b_1)\lambda + a_0 + b_0 = 0. \tag{12}$$

By Routh-Hurwitz criterion we know that all solutions of (12) have negative real parts if and only if

$$\begin{aligned}
H_1 =& a_3(a_2 + b_2) - (a_1 + b_1) > 0,\\
H_2 =& a_3(a_2 + b_2)(a_1 + b_1) - a_3^2(a_0 + b_0) - (a_1 + b_1)^2 > 0.
\end{aligned} \tag{13}$$

The stability is given in the following theorem.

**Theorem 3.3.** *If $R_0 > 1$ and $\tau = 0$, then the infected steady state $P_*$ of model (3) is locally asymptotically stable provided that (13) holds.*

The root of (11) depends on $\tau$ continuously [38]. All roots of (11) locate in the left side of the imaginary axis if $\tau = 0$ since the endemic equilibrium $P_*$ is stable. A root of (11) may pass through the imaginary axis and enter the right side when $\tau$ increases. $\lambda = i\omega$ is the critical case since a root may enter the right side or the left side under small perturbation when it locates on the imaginary axis. After substituting $\lambda = i\omega$ into (11) and separating the real and imaginary parts, we have

$$\begin{cases}
-\omega^4 + a_2\omega^2 - a_0 = (b_0 - b_2\omega^2)\cos\omega\tau + b_1\omega\sin\omega\tau,\\
-a_3\omega^3 + a_1\omega = (b_0 - b_2\omega^2)\sin\omega\tau - b_1\omega\cos\omega\tau.
\end{cases} \tag{14}$$

The equations of (14) lead to

$$G(z) = z^4 + D_1 z^3 + D_2 z^2 + D_3 z + D_4 = 0, \ z = \omega^2, \tag{15}$$

where $D_1 = a_3^2 - 2a_2$, $D_2 = a_2^2 + 2a_0 - 2a_1a_3 - b_2^2$, $D_3 = a_1^2 - 2a_2a_0 + 2b_2b_0 - b_1^2$, and $D_4 = a_0^2 - b_0^2$. $F(\lambda, \tau) = 0$ has a purely imaginary root $i\omega$ is equivalent to that $G(z) = 0$ has a positive real root $z$.

From the definition of $G(z)$, we have $G'(z) = 4z^3 + 3D_1z^2 + 2D_2z + D_3$. If we introduce $y = z + \frac{3D_1}{4}$, then we know that $G'(z) = 0$ is equivalent to $y^3 + m_1y + m_2 =$

0, where $m_1 = \frac{D_2}{2} - \frac{3}{16}D_1^2$, $m_2 = \frac{D_1^3}{32} - \frac{D_1 D_2}{8} + D_3$. Define

$$\begin{aligned}
\Delta =& \left(\frac{m_2}{2}\right)^2 + \left(\frac{m_1}{3}\right)^3, \ \sigma = \frac{-1+\sqrt{3}i}{2},\\
y_1 =& \sqrt[3]{-\frac{m_2}{2} + \sqrt{\Delta}} + \sqrt[3]{-\frac{m_2}{2} - \sqrt{\Delta}},\\
y_2 =& \sqrt[3]{-\frac{m_2}{2} + \sqrt{\Delta}\sigma} + \sqrt[3]{-\frac{m_2}{2} - \sqrt{\Delta}\sigma^2},\\
y_3 =& \sqrt[3]{-\frac{m_2}{2} + \sqrt{\Delta}\sigma^2} + \sqrt[3]{-\frac{m_2}{2} - \sqrt{\Delta}\sigma},\\
z_i =& y_i - \frac{3D_1}{4}, \ i = 1, 2, 3.
\end{aligned}$$

From [39], we have

**Lemma 3.4.** *For the polynomial equation $G(z) = 0$*

*(i) If $D_4 < 0$, then $G(z) = 0$ has at least one positive root;*
*(ii) If $D_4 \geq 0$ and $\Delta \geq 0$, then $G(z) = 0$ has positive roots if and only if $z_1 > 0$ and $G(z_1) < 0$;*
*(iii) If $D_4 > 0$, and $\Delta < 0$, then $G(z) = 0$ has positive roots if and only if there exists at least one $z_* \in \{z_1, z_2, z_3\}$ such that $z_* > 0$ and $G(z_*) \leq 0$.*

Without loss of generality, we assume that $G(z) = 0$ has four positive roots, denote by $z_i^* (i = 1, 2, 3, 4)$. Let $\omega_i = \sqrt{z_i^*}$ $(i = 1, 2, 3, 4)$, and we have

$$\begin{aligned}
\cos(\omega_i \tau) =& G_1 = \frac{(\omega^4 - a_2\omega^2 + a_0)(b_2\omega^2 - b_0) + b_1\omega(a_3\omega^3 - a_1\omega)}{b_1^2\omega^2 + (b_0 - b_2\omega^2)^2},\\
\sin(\omega_i \tau) =& G_2 = \frac{b_1\omega(-\omega^4 + a_2\omega^2 - a_0) + (b_0 - b_2\omega^2)(-a_3\omega^3 + a_1\omega)}{b_1^2\omega^2 + (b_0 - b_2\omega^2)^2}.
\end{aligned}$$

Define

$$\tau_j^{(k)} = \begin{cases} \frac{1}{\omega_k}[\arccos(G_1) + 2\pi j], & G_2 \geq 0,\\ \frac{1}{\omega_k}[2\pi - \arccos(G_1) + 2\pi j], & G_2 < 0, \end{cases}$$

where $k = 1, 2, 3, 4$, $j = 0, 1, 2, \cdots$.

Let

$$\tau_0 = \tau_{j_0}^{(k_0)} = \min_{1 \leq k \leq 4, j \geq 0} \{\tau_j^{(k)}\}, \ \omega_0 = \omega_{k_0}, \ z_0 = z_{k_0}^*. \tag{16}$$

**Lemma 3.5.** *Suppose that the condition (13) holds.*

*(i) All roots of (11) have negative real parts for $\tau \in [0, \tau_0)$ if any one of the following conditions holds:*
  *(a) $D_4 < 0$;*
  *(b) $D_4 \geq 0$, $\Delta < 0$, $z_1 > 0$ and $G(z_1) < 0$;*
  *(c) $D_4 \geq 0$, $\Delta < 0$, there exists a $z_* \in \{z_1, z_2, z_3\}$ such that $z_* > 0$ and $G(z_*) \leq 0$.*
*(ii) All roots of (11) have negative real parts for $\tau \geq 0$ if the conditions in (i) are not satisfied.*

If $\lambda(\tau) = \alpha(\tau) + i\beta(\tau)$ is the pure imaginary root of characteristic equation (11), then $\alpha\left(\tau_j^{(k)}\right) = 0$ and $\beta\left(\tau_j^{(k)}\right) = \omega_k$ (k=1,2,3,4).

**Lemma 3.6.** *If $G'(z_k) \neq 0$, then $\frac{d\left(Re\lambda(\tau_j^{(k)})\right)}{d\tau} \neq 0$, and the sign of $\frac{d\left(Re\lambda(\tau_j^{(k)})\right)}{d\tau}$ is the same as that of $G'(z_k)$.*

*Proof.* Differentiating (11) with respect to $\tau$, we get

$$(4\lambda^3 + 3a_3\lambda^2 + 2a_2\lambda + a_1)\frac{d\lambda}{d\tau} + e^{-\lambda\tau}(2b_2\lambda + b_1)\frac{d\lambda}{d\tau} - e^{-\lambda\tau}(b_2\lambda^2 + b_1\lambda + b_0)\left(\tau\frac{d\lambda}{d\tau} + \lambda\right) = 0,$$

and

$$\begin{aligned}\left(\frac{d\lambda}{d\tau}\right)^{-1} =& \frac{4\lambda^3 + 3a_3\lambda^2 + 2a_2\lambda + a_1}{\lambda e^{-\lambda\tau}(b_2\lambda^2 + b_1\lambda + b_0)} + \frac{2b_2\lambda + b_1}{\lambda(b_2\lambda^2 + b_1\lambda + b_0)} - \frac{\tau}{\lambda} \\ =& \frac{4\lambda^3 + 3a_3\lambda^2 + 2a_2\lambda + a_1}{-\lambda(\lambda^4 + a_3\lambda^3 + a_2\lambda^2 + a_1\lambda + a_0)} + \frac{2b_2\lambda + b_1}{\lambda(b_2\lambda^2 + b_1\lambda + b_0)} - \frac{\tau}{\lambda}.\end{aligned}$$

The fact $\operatorname{sign}\left\{\frac{d(\mathrm{Re}\lambda)}{d\tau}\Big|_{\tau=\tau_j^{(k)}}\right\} = \operatorname{sign}\left\{\mathrm{Re}\left(\frac{d\lambda}{d\tau}\right)^{-1}\right\}_{\lambda=i\omega_k}$ leads to

$$\begin{aligned}&\operatorname{sign}\left\{\frac{d(\mathrm{Re}\lambda)}{d\tau}\right\}\Big|_{\tau=\tau_j^{(k)}} \\ =&\operatorname{sign}\left\{\mathrm{Re}\left[\frac{4\lambda^3 + 3a_3\lambda^2 + 2a_2\lambda + a_1}{-\lambda(\lambda^4 + a_3\lambda^3 + a_2\lambda^2 + a_1\lambda + a_0)}\right]\Big|_{\lambda=i\omega_k}\right. \\ &\left. + \mathrm{Re}\left[\frac{2b_2\lambda + b_1}{\lambda(b_2\lambda^2 + b_1\lambda + b_0)}\right]\Big|_{\lambda=i\omega_k}\right\} \\ =&\operatorname{sign}\left\{\frac{(4\omega_k^3 - 2a_2\omega_k)(\omega_k^4 - a_2\omega_k^2 + a_0) + (a_1 - 3a_3\omega_k^2)(a_1\omega_k - a_3\omega_k^3)}{\omega_k[(\omega_k^4 - a_2\omega_k^2 + a_0)^2 + (a_1\omega_k - a_3\omega_k^3)^2]}\right. \\ &\left. + \frac{2b_2\omega_k(b_2\omega_k^2 - b_0) + b_1^2\omega_k}{w[(b_2\omega_k^2 - b_0)^2 + b_1^2\omega_k^2]}\right\} \\ =&\operatorname{sign}\left\{\frac{4\omega_k^6 + 3D_1\omega_k^4 + 2D_2\omega_k^2 + D_3}{(b_2\omega_k^2 - b_0)^2 + b_1^2\omega_k^2}\right\} \\ =&\operatorname{sign}\left\{\frac{G'(\omega_k^2)}{(b_2\omega_k^2 - b_0)^2 + b_1^2\omega_k^2}\right\} \\ =&\operatorname{sign}\left\{\frac{G'(z_k)}{(b_2\omega_k^2 - b_0)^2 + b_1^2\omega_k^2}\right\}.\end{aligned}$$

The obvious fact $(b_2\omega_k^2 - b_0)^2 + b_1^2\omega_k^2 > 0$ yields

$$\operatorname{sign}\left\{\frac{d\left(\mathrm{Re}\lambda(\tau_j^{(k)})\right)}{d\tau}\right\} = \operatorname{sign}\{G'(z_k)\}. \tag{17}$$

This completes the proof of the Lemma. □

According to the Hopf bifurcation theorem for functional differential equations [40, Theorem 1.1 in Chapter 11] and together with Lemmas 3.4, 3.5 and 3.6 we have following result.

**Theorem 3.7.** *Let $\tau_0$, $z_0$ be defined by (16). Suppose that (13) holds.*

*(i) If the conditions of (a)–(c) of Lemma 3.5 are not satisfied, then infected steady state $P_*$ is asymptotically stable for all $\tau \geq 0$.*

*(ii) If one of the conditions (a)–(c) of Lemma 3.5 is satisfied, then the infected steady state $P_*$ is asymptotically stable for $\tau \in [0, \tau_0)$.*

*(iii) If one of the conditions (a)–(c) of Lemma 3.5 holds, and $G'(z_k) \neq 0$, then model (3) undergoes a Hopf bifurcation at the infected steady state $P_*$ when $\tau = \tau_j^{(k)}$.*

3.3. **Direction and stability of Hopf bifurcations.** In this subsection, we study the direction and stability of the Hopf bifurcation by using the normal theory and the center manifold theorem [41]. We always assume that model (3) undergoes Hopf bifurcation at the steady state $P_* = (T_*, I_*, V_*, E_*)$ for $\tau = \tilde{\tau} = \tau_j^{(k)}$. Let $i\omega$ be the purely imaginary roots of the characteristic equation at the infected steady state $P_* = (T_*, I_*, V_*, E_*)$ for $\tau = \tilde{\tau}$. The conditions for direction and stability of Hopf bifurcation are summarized in the following theorem.

**Theorem 3.8.** *(i) The direction of Hopf bifurcation is determined by the sign of $\mu_2$: if $\mu_2 > 0$, then it is a supercritical bifurcation; if $\mu_2 < 0$, then it is a subcritical bifurcation. (ii) The stability of the bifurcated periodic solution is determined by $\overline{\beta}_2$: the periodic solution is stable if $\overline{\beta}_2 < 0$, and it is unstable if $\overline{\beta}_2 > 0$. (iii) The period of bifurcated periodic solutions is determined by $T_2$: the period increases if $T_2 > 0$, and it decreases if $T_2 < 0$. Where*

$$
\begin{aligned}
c_1(0) &= \frac{i}{2\omega\tilde{\tau}}\left(g_{20}g_{11} - 2|g_{11}|^2 - \frac{|g_{02}|^2}{3}\right) + \frac{g_{21}}{2},\\
\mu_2 &= -\frac{Re\{c_1(0)\}}{Re\{\lambda'(\tilde{\tau})\}},\\
\overline{\beta}_2 &= 2Re(c_1(0)),\\
T_2 &= -\frac{Im(c_1(0)) + \mu_2 Im(\lambda'(\tilde{\tau}))}{\omega\tilde{\tau}}.
\end{aligned}
$$

The detailed calculation of $\mu_2$, $\overline{\beta}_2$ and $T_2$ is given in Appendix A.

TABLE 1. List of parameters.

| Parameters | Range of parameters | Source | Data1 | Data2 |
|---|---|---|---|---|
| $s$ | 0–10 cells mm$^{-3}$ day$^{-1}$ | [2, 6, 8, 14] | 10 | 10 |
| $d$ | 0.007–0.1 day$^{-1}$ | [8, 14] | 0.1 | 0.01 |
| $\beta_1$ | 0.00025–0.5 virons mm$^3$ day$^{-1}$ | [2, 6, 14] | 0.00025 | 0.00025 |
| $\beta_2$ | – | Assumed | 0.00065 | 0.00065 |
| $r$ | 0.03–3 day$^{-1}$ | [2, 6, 14] | 0.03 | 0.1 |
| $T_{max}$ | 1500 mm$^{-3}$ | [6, 14] | 1500 | 1500 |
| $\alpha$ | $\geq 1$ | [32] | 1.2 | 1.2 |
| $d_1$ | 0.2–0.5 day$^{-1}$ | [6, 14] | 0.5 | 0.4 |
| $d_2$ | 2.4–3 day$^{-1}$ | [6, 14] | 3 | 2.4 |
| $d_3$ | 0.812 day$^{-1}$ | [3] | 0.812 | 0.812 |
| $d_4$ | 1.618 day$^{-1}$ | [3] | 0.618 | 1.618 |
| $N$ | 10–2500 virons/cell | [2, 14] | 50 | 500 |
| $p$ | 0.05 day$^{-1}$ | [5] | 0.05 | 0.05 |

4. **Numerical simulation.** Numerical simulations are done to illustrate the dynamical behaviors of model (3) for different $\tau$. The other parameter values in the simulation are listed in Table 1.

For the parameter values Data 1 given in Table.1. It is easy to see that $R_0 = 0.7514 < 1$, from Theorem 3.2 shows that the infection-free steady state $P_0$ is globally asymptotically stable for any $\tau \geq 0$ (see Fig. 1)

Under the condition (13) the infected steady state $P_*$ is locally asymptotically stable independent of the size of the delay, though the time delay does cause transient oscillations in all components. For the parameter values given in the last column of Table 1, we can compute that $R_0 = 78.05 > 1$ and the infected steady state is $P_* = (37.71854, 16.3522, 1362.6799, 0.5053)$. The positive real roots of (15) are $z_1 = 0.3563$, $z_2 = 0.1039$, and the pure imaginary roots of (11) are $\lambda_1 = i\omega_1$ and $\lambda_2 = i\omega_2$ with $\omega_1 = 0.5969 > \omega_2 = 0.3223$. Furthermore, we have $G'(z_1) > 0$ and $G'(z_2) < 0$. From the transversal condition (17) and [15], we can have following results.

(a) At $\tau_j^{(1)}$, $j = 0, 1, 2, \cdots$, a pair of characteristic roots of (11) crosses the imaginary axis from left to the right.

(b) At $\tau_j^{(2)}$, $j = 0, 1, 2, \cdots$, a pair of characteristic roots of (11) crosses the imaginary axis from right to the left.

(c) $\tau_j^{(1)} - \tau_{j-1}^{(1)} = \frac{2\pi}{\omega_1} < \frac{2\pi}{\omega_2} = \tau_j^{(2)} - \tau_{j-1}^{(2)}$.

From (c) we know that there exists an integer $k$ such that $\tau_j^{(1)}$ and $\tau_j^{(2)}$ satisfy

$$\tau_0^{(1)} < \tau_0^{(2)} < \tau_1^{(1)} < \tau_1^{(2)} < \cdots < \tau_k^{(1)} < \tau_{k+1}^{(1)} < \tau_k^{(2)}.$$

The results of (a)–(c) imply the stability switch as $\tau$ increases: a pair of characteristic roots will cross the imaginary axis to the right at $\tau_0^{(1)}$ and get back to the left at $\tau_0^{(2)}$. The stability switch continues until for a $\tau = \tau_k^{(1)}$ when a pair of characteristic roots crosses the imaginary axis from left to the right and remains in the right. The two sequences given by numerical simulations are

$$\{\tau_j^{(1)}\}_{j=0}^{\infty} = \{2.5901, 13.1167, 23.6433, 34.1700, \cdots\},$$
$$\{\tau_j^{(2)}\}_{j=0}^{\infty} = \{10.2828, 29.7767, 49.2706, \cdots\}.$$

Furthermore, there exists a $k = 1$ such that $\tau_0^{(1)} < \tau_0^{(2)} < \tau_1^{(1)} < \tau_2^{(1)} < \tau_1^{(2)}$. The infected steady state $P_*$ is stable for $\tau < 2.5901$, unstable for $\tau \in (2.5901, 10.2828)$, stable for $\tau \in (10.2828, 13.1167)$, and unstable for $\tau > 13.1167$, which is presented in Fig. 2 and the corresponding stability and bifurcation is shown in Fig. 3 (left). The horizontal axis is the delay $\tau$, and the vertical axis is the virus $V$. For $\tau < 2.5901$ and $\tau \in (10.2828, 13.1167)$, there is a line in Fig. 3 (left), which is given $V = V_* = 1362.6799$, the infected steady state $P_*$ is locally asymptotically stable. For $\tau \in (2.5901, 10.2828)$, when $\tau$ cross $\tau_0^{(1)}$, we can compute $c_1(0) = -0.2072941082433112 - 1.037904500371602 \times 10^2 i$, $\mu_2 = 3.959023703656483 > 0$, $\bar{\beta}_2 = -0.414588216486622 < 0$ and $T_2 = 67.303256908139844 > 0$. Hence, Theorem 3.8 implies that there exists a stable periodic solution of model (3). The two curves in Fig. 3 are the maximal and minimal values of $V(t)$ in a period. Similarly, when $\tau$ cross $\tau_1^{(1)}$, we can compute $c_1(0) = -0.470254201495353 - 94.354228525286175i$, $\mu_2 = 47.973638016773599 > 0$, $\bar{\beta}_2 = -0.940508402990705 < 0$ and $T_2 = 12.261483017883963 > 0$, thus, there also exists stable periodic solutions of model (3) for $\tau > 13.1167$. Fig. 4 shows that when $\tau = 31$, chaotic motions occurs. Furthermore, from Fig. 5, when $\tau$ becomes large, say $\tau = 49$, the infected steady state $P_*$ is unstable, and the system trajectory exhibits a transient seemingly chaotic solution for a longer time (see the small figures in Fig. 5) then involves into

a final nonchaotic state such as a quasi-periodic solution. Thus, immune response delay has an effect on the control of the disease.

From Fig. 6, which shows that though the components $I$ and $V$ of the infection steady state are only slightly changed, the time needed for the system converge to the steady state is much shorter as $\beta_2$ increases, i.e. the system will spend a shorter time to reach the steady state for high value of $\beta_2$. Moreover, the figures in Fig. 7 together with the Fig. 3 (left one) shows that the stable intervals is enlarged as $\beta_2$ increases, though the amplitude of the periodic solutions is smaller. And when $\beta_2 = 0.01$, the Fig. 7 (right) shows that multiple stability switches can occurs. Hence, neglecting cell-to-cell transmission ($\beta_2$) may lose some dynamics behavior. As for parameter $s$, which is the source of new health target cells from precursors. Fig. 8, shows that the components $I$ and $V$ of the infection steady state increases as $s$ increases. This is because high value of $s$ increases the pool of susceptible target cells. Moreover, comparing with Fig. 9 and Fig. 3 (left) we can see that the amplitude of the periodic solutions increases as $s$ increases, but the stable interval decreases. Furthermore, numerical simulation shows that there is a period-doubling solution (see Fig. 10). From Fig. 11, we can see that the component $I$ and $V$ of the infection steady state decreases as $d$ increases. Comparing with Fig. 3 (left) and Fig. 12, we can see that the amplitude of the periodic solutions decreases as $d$ increases, whereas the length of the stable interval increases. Hence, both the recruitment rate $s$ and the death rate $d$ of the target cells do have some impact on the dynamics of the model.

In general, the existence of logistic term may lead to rich dynamics for a model, especially for a model without delay, logistic term may cause Hopf bifurcation. In order to show the impact of the delay on the dynamics of the model without the effect of logistic term. Then, we give the bifurcation diagram when the system is in absence of logistic term, i.e., $r = 0$ in Fig. 3 (right), which implies that stability switch and Hopf bifurcation still exist when there is no logistic growth term for the system. Thus, we can see that stability switch, Hopf bifurcation and chaotic oscillation exist in both cases. We can claim that when take immune responses into consideration, time delay may be the main factor for periodic oscillations. Furthermore, the two figures in Fig. 3 show that the stable intervals for the system in absence of logistic growth term is much larger than the system with logistic growth term and the oscillation interval will be enlarged as $r$ increases, though the existence of logistic growth term may not change the main dynamics behavior of the system.

Simulations are also done to show the impact of logistic growth term $r$ on the dynamics of the model (see Fig. 13 and Fig. 14). The simulation shows that the infected steady state $P_*$ may be stable or unstable, and the model may has periodic solutions, or chaotic motions, depending on $r$. From Fig. 13, we see that only Hopf bifurcation occurs and no chaotic motions when $\tau$, say $\tau = 2$, stay in a stable interval; while both hopf bifurcation and chaotic motions exist when $\tau$, say $\tau = 5$, stay in an unstable interval, and the corresponding bifurcation diagrams are given in Fig. 14, respectively. Moreover, Fig. 14 (left) shows that at the left end of the $r$ range, though there exists an interval for which the infected steady state $P_*$ is asymptotically stable, the viral load increases, then Hopf bifurcation occurs and the amplitude of the bifurcating periodic solutions increase and then decrease as $r$ increase. Thus, the simulation shows that the logistic growth term also plays an important role on the dynamics of the model. Our results suggest that both immune

delay and logistic growth term are responsible for rich dynamics of the model.

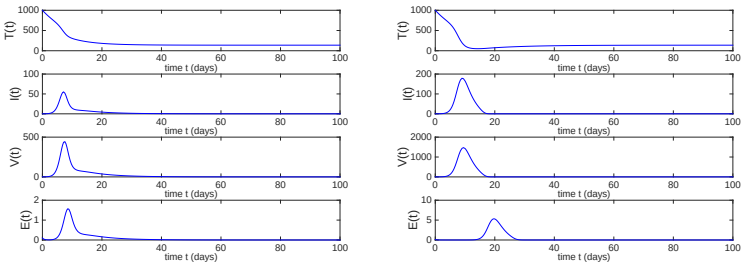


FIGURE 1. $P_0$ is globally asymptotically stable for $\tau = 1$ (left) and $\tau = 10$ (right).

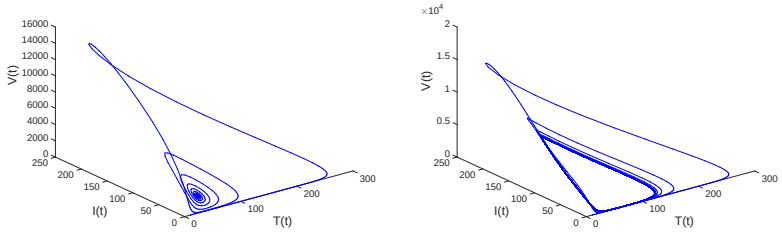


(a) $\tau = 2$ (b) $\tau = 5$

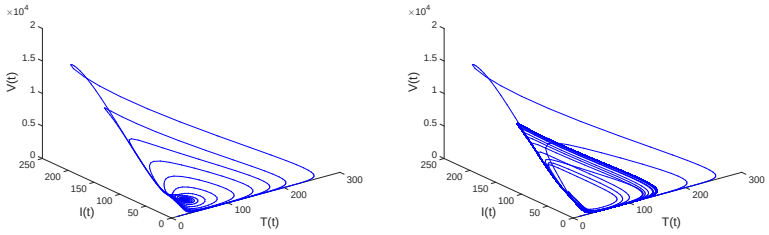


(c) $\tau = 12$ (d) $\tau = 25$

FIGURE 2. Solutions of model (3) for different $\tau$.

5. **Summary and discussion.** In this paper, we extend the previous work to a more realistic delayed model including cell-to-cell transmission. The basic reproduction number $R_0$ include two parts: cell-to-cell infection and virus-to-cell infection. It is easy to see that the basic reproduction number will be underestimated for models neglecting the cell-to-cell infection or virus-to-cell infection. Mathematical analysis gives the conditions for the existence of the equilibria and shows the influence of the time delay on the stability of equilibrium states. It is proved that the local stability of the uninfected steady state is independent of the size of the delay. Furthermore, the global stability of the uninfected steady state $P_0$ is obtained if $R_0$ is less than one by applying the fluctuation lemma. Our results show that

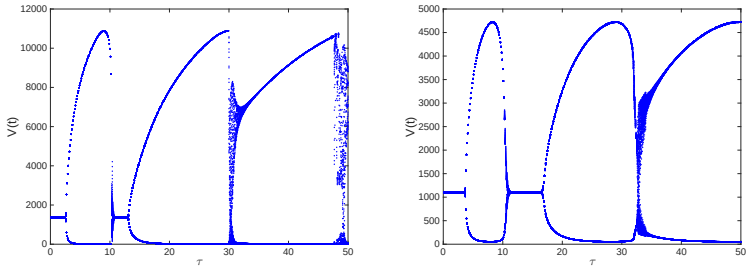


FIGURE 3. The stability and bifurcation for $r = 0.1$ (left) and $r = 0$ (right).

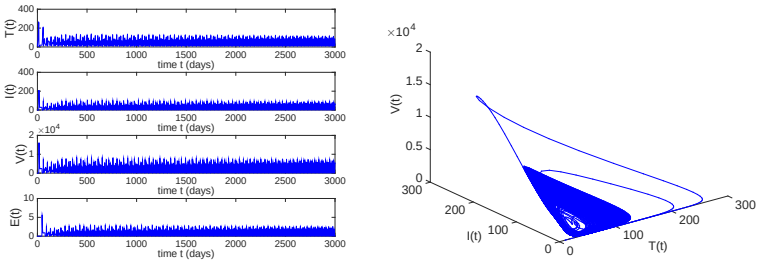


FIGURE 4. Solutions of model (3) for $\tau = 31$.

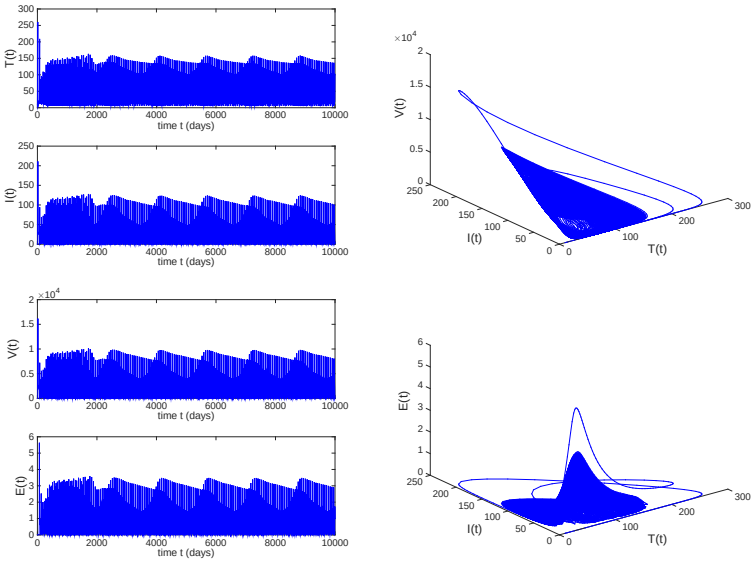


FIGURE 5. Solutions of model (3) for $\tau = 49$.

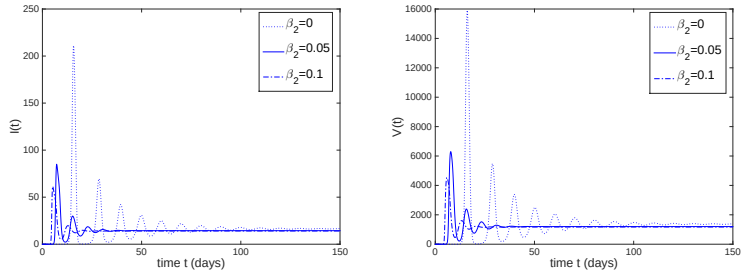


FIGURE 6. Solutions of model (3) for different values of $\beta_2$ with $\tau = 2$.

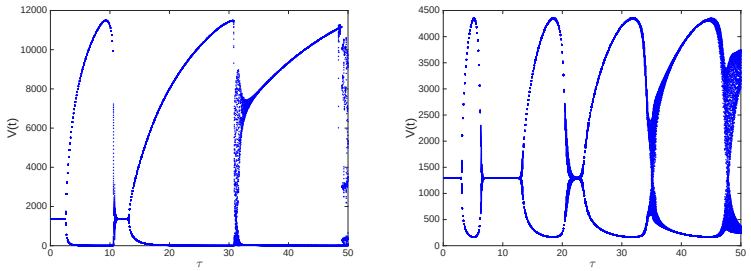


FIGURE 7. The stability and bifurcation with $\beta_2 = 0$ (left) and $\beta_2 = 0.01$ (right).

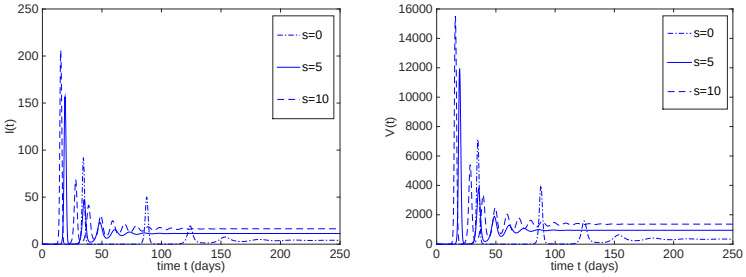


FIGURE 8. The effects of $s$ on the system with $\tau = 2$.

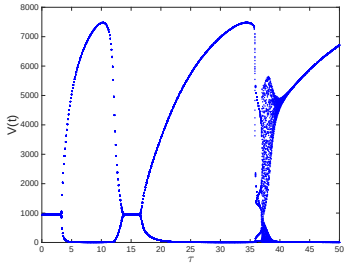


FIGURE 9. The stability and bifurcation with $s = 5$.

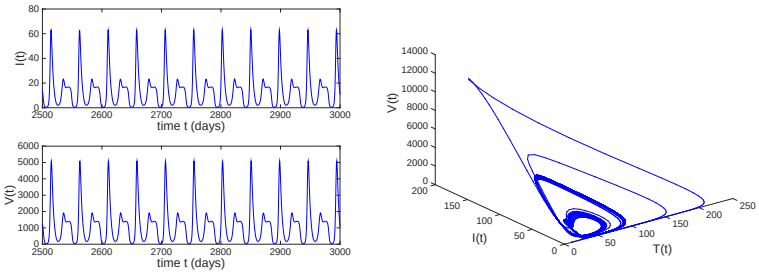


FIGURE 10. There exists a period-doubling solution with $s = 5, \tau = 36$.

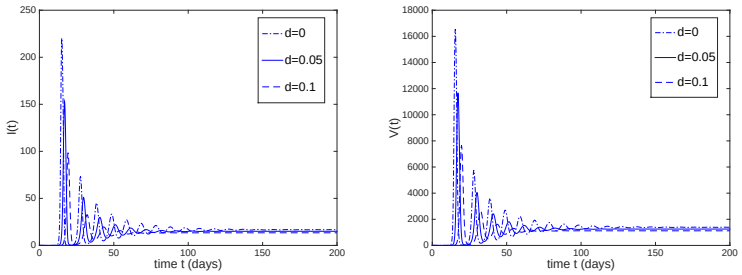


FIGURE 11. The effects of $d$ on the system with $\tau = 2$.

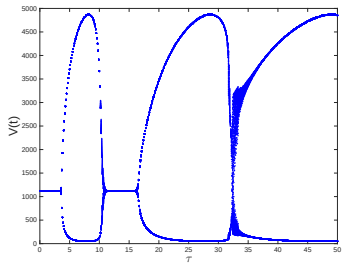


FIGURE 12. The stability and bifurcation with $d = 0.1$.

increasing the delay can destabilize the infected steady state by leading to a Hopf bifurcation and periodic solutions. The bifurcation direction and the stability of the periodic solutions are investigated by using normal form and center manifold. The theoretical analysis shows the importance of time delay on HIV dynamics.

Numerical simulations show that both cell-to-cell transmission and time delay $\tau$ have an impact on the dynamics of the model, and rich dynamics can occur for large $\tau$ in the realistic parameter space. Compared to the earlier studies [3, 32], our analysis shows that the introduction of the immune delay not only destabilize the stability of the infected steady state, leading to a Hopf bifurcation and periodic solutions, but also stability switch occurs as time delay $\tau$ increases, which has not been observed in [3, 16, 32]. Chaotic oscillations were observed for large $\tau$. We also

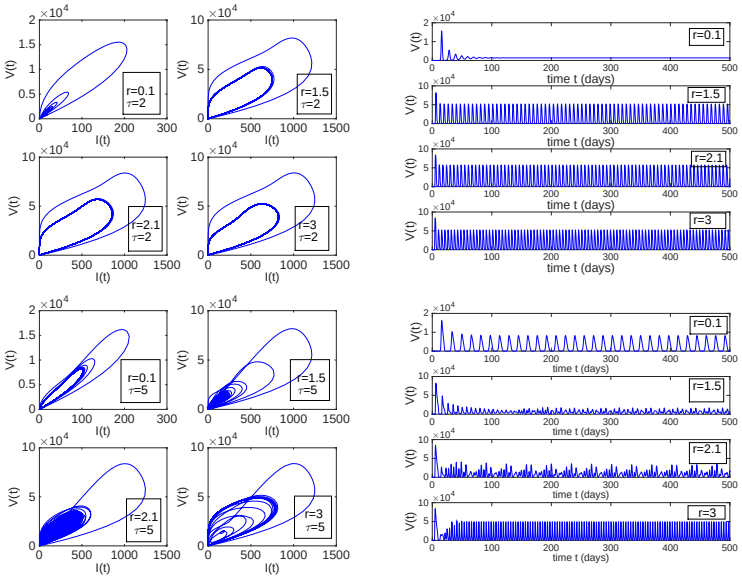


FIGURE 13. Solutions of model (3) for $r = 0.1, 1.5, 2.1, 3$, with $\tau = 2$ (top plots) and $\tau = 5$ (bottom plots).

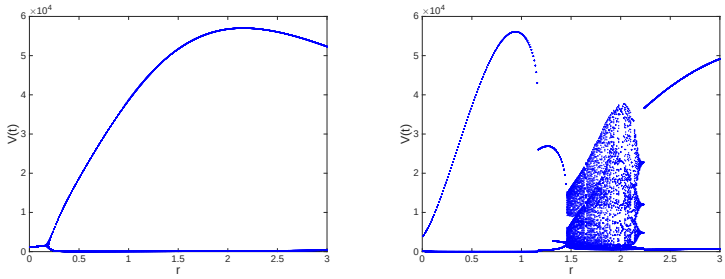


FIGURE 14. The stability and bifurcation of (3) with $\tau = 2$ (left) and $\tau = 5$ (right).

find that the viral load may be destabilized into oscillations with the increase of the logistic growth rate $r$ for T-cells. Moreover, numerical simulations also show that the oscillation interval will be enlarged as $r$ increases. The system can occurs multiple stability switches for high value of cell-to-cell transmission $\beta_2$, and the stable intervals is larger though the amplitude is smaller. Furthermore, numerical simulations show that larger $\beta_2$ makes the system converge to the steady state more easily. Hence, our results suggest that the logistic growth rate for T-cells $r$ and the immune response delay $\tau$ and the cell-to-cell transmission are responsible for the complex dynamics.

Although the delay of immune response and cell-to-cell transmission considered in this paper is a good way to improve the viral dynamic model, the intracellular delays should also be taken into consideration for more realistic models. The dynamical analysis of the epidemic models with multiple delays will be more complex and bigger challenge in the future.

**Appendix** A. **Proof of Theorem 3.8.** We use the variable transformations

$$x_1(t) = T(\tau t) - T_*,\ x_2(t) = I(\tau t) - I_*,\ x_3(t) = V(\tau t) - V_*,$$
$$x_4(t) = E(\tau t) - E_*, \tau = \tilde{\tau} + \mu$$

to make model (3) become an functional differential equation in $C = C([-1, 0], \mathbb{R}^4)$.

$$\frac{dx}{dt} = L_\mu(x_t) + f(\mu, x_t), \tag{18}$$

where $x(t) = (x_1(t), x_2(t), x_3(t), x_4(t))^T \in \mathbb{R}^4$ , $L_\mu : C \to \mathbb{R}^4$, and $f : \mathbb{R} \times C \to \mathbb{R}^4$,

$$L_\mu(\phi) = (\tilde{\tau} + \mu)B_1\phi(0) + (\tilde{\tau} + \mu)B_2\phi(-1), \tag{19}$$

$$\begin{aligned} &f(\mu, \phi) \\ =&(\tilde{\tau} + \mu) \begin{pmatrix} -\frac{r}{T_{max}}\phi_1^2(0) - \left(\frac{\alpha r}{T_{max}} + \beta_2\right)\phi_1(0)\phi_2(0) - \beta_1\phi_1(0)\phi_3(0) \\ \beta_1\phi_1(0)\phi_3(0) + \beta_2\phi_1(0)\phi_2(0) - d_3\phi_2(0)\phi_4(0) \\ 0 \\ 0 \end{pmatrix}, \end{aligned} \tag{20}$$

with $\phi(\theta) = (\phi_1(\theta), \phi_2(\theta), \phi_3(\theta), \phi_4(\theta))^T \in C$ and

$$B_1 = \begin{pmatrix} -\left(\frac{rT_*}{T_{max}} + \frac{s}{T_*}\right) & -\left(\frac{\alpha r T_*}{T_{max}} + \beta_2 T_*\right) & -\beta_1 T_* & 0 \\ \beta_1 V_* + \beta_2 I_* & -\beta_1 \frac{N d_1}{d_2} T_* & \beta_1 T_* & -d_3 I_* \\ 0 & N d_1 & -d_2 & 0 \\ 0 & 0 & 0 & -d_4 \end{pmatrix},$$

$$B_2 = \begin{pmatrix} 0 & 0 & 0 & 0 \\ 0 & 0 & 0 & 0 \\ 0 & 0 & 0 & 0 \\ 0 & p & 0 & 0 \end{pmatrix}.$$

By Reisz representation theorem, there exists a matrix components, bounded variation function $\eta(\theta, \mu)$ in $\theta \in [-1, 0]$, such that $L_\mu\phi = \int_{-1}^{0} d\eta(\theta, \mu)\phi(\theta)$ for $\phi \in C$. In fact, we can choose

$$\eta(\theta, \mu) = (\tilde{\tau} + \mu)B_1\delta(\theta) - (\tilde{\tau} + \mu)B_2\delta(\theta + 1), \tag{21}$$

where, $\delta$ denote the Dirac delta function. For $\phi \in C^1([-1, 0], \mathbb{R}^4)$, define

$$A(\mu)\phi = \begin{cases} \frac{d\phi(\theta)}{d\theta}, & \theta \in [-1, 0), \\ \int_{-1}^{0} d\eta(\mu, s)\phi(s), & \theta = 0, \end{cases}$$

and

$$R(\mu)\phi = \begin{cases} 0, & \theta \in [-1, 0), \\ f(\mu, \phi), & \theta = 0. \end{cases}$$

Model (18) is equivalent to

$$\dot{x_t} = A(\mu)x_t + R(\mu)x_t,\ x_t = x(t + \theta),\ \theta \in [-1, 0]. \tag{22}$$

For $\psi \in C^1([0, 1], (\mathbb{R}^4)^*)$, define

$$A^*\psi(s) = \begin{cases} -\frac{d\psi(s)}{ds}, & s \in (0, 1], \\ \int_{-1}^{0} d\eta^T(s, 0)\psi(-s), & s = 0, \end{cases}$$

and a bilinear inner product

$$\langle \psi, \phi \rangle = \bar{\psi}(0)\phi(0) - \int_{-1}^{0}\int_{\xi=0}^{\theta} \bar{\psi}(\xi-\theta)d\eta(\theta)\phi(\xi)d\xi, \tag{23}$$

where $\eta(\theta) = \eta(\theta, 0)$. Then $A(0)$ and $A^*$ are adjoint operators with eigenvalues $\pm i\omega\tilde{\tau}$. We compute the eigenvector of $A(0)$ and $A^*$ corresponding to $i\omega\tilde{\tau}$ and $-i\omega\tilde{\tau}$, respectively. If $q(\theta) = (1, q_1, q_2, q_3)^T e^{i\theta\omega\tilde{\tau}}$ is the eigenvector of $A(0)$ corresponding to $i\omega\tilde{\tau}$, then $A(0)q(\theta) = i\omega\tilde{\tau}q(\theta)$, and

$$\tilde{\tau}\begin{pmatrix} i\omega + \frac{rT_*}{T_{max}} + \frac{s}{T_*} & \frac{\alpha r T_*}{T_{max}} + \beta_2 T_* & \beta_1 T_* & 0 \\ -(\beta_1 V_* + \beta_2 I_*) & i\omega + \beta_1 \frac{Nd_1}{d_2} T_* & -\beta_1 T_* & d_3 I_* \\ 0 & -\delta & i\omega + d_2 & 0 \\ 0 & -pe^{-i\omega\tilde{\tau}} & 0 & i\omega + d_4 \end{pmatrix}\begin{pmatrix} 1 \\ q_1 \\ q_2 \\ q_3 \end{pmatrix} = \begin{pmatrix} 0 \\ 0 \\ 0 \\ 0 \end{pmatrix}.$$

We can obtain

$$\begin{aligned} q_1 =& -\frac{(i\omega + d_2)\left(i\omega + \frac{rT_*}{T_{max}} + \frac{s}{T_*}\right)}{(i\omega + d_2)\left(\beta_2 T_* + \frac{\alpha r T_*}{T_{max}}\right) + \beta_1 N d_1 T_*}, \\ q_2 =& \frac{Nd_1 q_1}{i\omega + d_2},\ q_3 = \frac{pe^{-i\omega\tilde{\tau}}}{i\omega + d_4}. \end{aligned}$$

On the other hand, if $q^*(s) = D(1, q_1^*, q_2^*, q_3^*)e^{is\omega\tilde{\tau}}$ is the eigenvector of $A^*$ corresponding to $-i\omega\tilde{\tau}$, then we have

$$\tilde{\tau}\begin{pmatrix} -i\omega + \frac{rT_*}{T_{max}} + \frac{s}{T_*} & -(\beta_1 V_* + \beta_2 I_*) & 0 & 0 \\ \frac{\alpha r T_*}{T_{max}} + \beta_2 T_* & -i\omega + \beta_1 \frac{Nd_1}{d_2} T_* & -\delta & -pe^{i\omega\tilde{\tau}} \\ \beta_1 T_* & -\beta_1 T_* & -i\omega + d_2 & 0 \\ 0 & d_3 I_* & 0 & -i\omega + d_4 \end{pmatrix}\begin{pmatrix} 1 \\ q_1^* \\ q_2^* \\ q_3^* \end{pmatrix} = \begin{pmatrix} 0 \\ 0 \\ 0 \\ 0 \end{pmatrix},$$

and

$$q_1^* = \frac{-i\omega + \frac{rT_*}{T_{max}} + \frac{s}{T_*}}{\beta_1 V_* + \beta_2 I_*},\ q_2^* = \frac{\beta_1 T_*(q_1^* - 1)}{-i\omega + d_2},\ q_3^* = \frac{d_3 I_* q_1^*}{i\omega - d_4}.$$

We can choose $D = \dfrac{1}{1 + \overline{q}_1 q_1^* + \overline{q}_2 q_2^* + \overline{q}_3 q_3^* + \tilde{\tau} p q_1 \overline{q}_3^* e^{i\omega\tilde{\tau}}}$ to have $\langle q^*(s), q(\theta)\rangle = 1$. By (23), we have

$$\begin{aligned} \langle q^*(s), q(\theta)\rangle =& \overline{D}(1, \overline{q}_1^*, \overline{q}_2^*, \overline{q}_3^*)(1, q_1, q_2, q_3)^T \\ & - \int_{-1}^{0}\int_{\xi=0}^{\theta} \overline{D}(1, \overline{q}_1^*, \overline{q}_2^*, \overline{q}_3^*)e^{-i(\xi-\theta)\omega\tilde{\tau}} d\eta(\theta)(1, q_1, q_2, q_3)^T e^{i\xi\omega\tilde{\tau}} d\xi \\ =& \overline{D}\left\{1 + q_1\overline{q}_1^* + q_2\overline{q}_2^* + q_3\overline{q}_3^* - \int_{-1}^{0}(1, q_1^*, q_2^*, q_3^*)\theta e^{i\theta\omega\tilde{\tau}} d\eta(\theta)(1, q_1, q_2, q_3)^T\right\} \\ =& \overline{D}\left\{1 + q_1\overline{q}_1^* + q_2\overline{q}_2^* + q_3\overline{q}_3^* + \tilde{\tau} p q_1 \overline{q}_3^* e^{-i\omega\tilde{\tau}}\right\}. \end{aligned}$$

Next, we use the same notations as in [41], and compute the center manifold $C_0$ at $\mu = 0$. Let $x_t$ be the solution of (22) for $\mu = 0$. Define

$$z(t) = \langle q^*, x_t\rangle,\ W(t, \theta) = x_t(\theta) - 2\mathrm{Re}\{z(t)q(\theta)\}. \tag{24}$$

On the center manifold $C_0$ we have

$$W(t, \theta) = W(z, \bar{z}, \theta) = W_{20}\frac{z^2}{2} + W_{11}(\theta)z\bar{z} + W_{02}(\theta)\frac{\bar{z}^2}{2} + \cdots, \tag{25}$$

where $z$ and $\bar{z}$ are local coordinates for center manifold $C_0$ in the direction $q^*$ and $\overline{q}^*$. Note that $W$ is real if $x_t$ is real. We only consider real solutions. For the solution $x_t \in C_0$ of (22) with $\mu = 0$, we have

$$\begin{aligned}\dot{z}(t) =& i\omega\tilde{\tau}z + \langle \overline{q}^*(\theta), f(0, W(z,\overline{z},\theta) + 2\mathrm{Re}\{zq(\theta)\})\rangle \\ =& i\omega\tilde{\tau}z + \overline{q}^*(0) f(0, W(z,\overline{z},0) + 2\mathrm{Re}\{zq(0)\}) \\ \triangleq& i\omega\tilde{\tau}z + \overline{q}^*(0) f_0(z,\overline{z}).\end{aligned}$$

We define

$$g(z,\overline{z}) = \overline{q}^*(0) f_0(z,\bar{z}) = g_{20}\frac{z^2}{2} + g_{11}z\bar{z} + g_{02}\frac{\overline{z}^2}{2} + g_{21}\frac{z^2\bar{z}}{2} + \cdots \tag{26}$$

and study the equation

$$\dot{z}(t) = i\omega\tilde{\tau}z + g(z,\overline{z}).$$

It follows from (24) and (25) that

$$\begin{aligned} x_t(\theta) &= (x_{1t}(\theta), x_{2t}(\theta), x_{3t}(\theta), x_{4t}(\theta))^T \\ &= W(t,\theta) + 2Re\{zq(\theta)\} \\ &= (1, q_1, q_2, q_3)^T e^{i\omega\tilde{\tau}\theta} z + (1, \overline{q}_1, \overline{q}_2, \overline{q}_3)^T e^{-i\omega\tilde{\tau}\theta}\overline{z} \\ &\quad + W_{20}\frac{z^2}{2} + W_{11}(\theta)z\overline{z} + W_{02}(\theta)\frac{\overline{z}^2}{2} + \cdots, \end{aligned} \tag{27}$$

and

$$\begin{aligned} x_{1t}(0) =& z + \overline{z} + W_{20}^{(1)}(0)\frac{z^2}{2} + W_{11}^{(1)}(0)z\overline{z} + W_{02}^{(1)}(0)\frac{\overline{z}^2}{2} + O(|(z,\overline{z})|^3), \\ x_{2t}(0) =& q_1 z + \overline{q}_1\overline{z} + W_{20}^{(2)}(0)\frac{z^2}{2} + W_{11}^{(2)}(0)z\overline{z} + W_{02}^{(2)}(0)\frac{\overline{z}^2}{2} + O(|(z,\overline{z})|^3), \\ x_{3t}(0) =& q_2 z + \overline{q}_2\overline{z} + W_{20}^{(3)}(0)\frac{z^2}{2} + W_{11}^{(3)}(0)z\overline{z} + W_{02}^{(3)}(0)\frac{\overline{z}^2}{2} + O(|(z,\overline{z})|^3), \\ x_{4t}(0) =& q_3 z + \overline{q}_3\overline{z} + W_{20}^{(4)}(0)\frac{z^2}{2} + W_{11}^{(4)}(0)z\overline{z} + W_{02}^{(4)}(0)\frac{\overline{z}^2}{2} + O(|(z,\overline{z})|^3). \end{aligned}$$

It follows from (20) that

$$\begin{aligned} g(z,\overline{z}) =& \overline{q}^*(0) f_0(z,\overline{z}) \\ =& \overline{q}^*(0) f_0(0, x_t) \\ =& \tilde{\tau}\overline{q}^*(0)\begin{pmatrix} -\frac{r x_{1t}^2(0)}{T_{max}} - \left(\frac{\alpha r}{T_{max}} + \beta_2\right) x_{1t}(0)x_{2t}(0) - \beta_1 x_{1t}(0)x_{3t}(0) \\ \beta_2 x_{1t}(0)x_{2t}(0) + \beta_1 x_{1t}(0)x_{3t}(0) - d_3 x_{2t}(0)x_{4t}(0) \\ 0 \\ 0 \end{pmatrix} \\ =& \tilde{\tau}\overline{D}\Big\{ -\frac{r}{T_{max}}x_{1t}^2(0) + \left(\overline{q}_1^*\beta_2 - \frac{\alpha r}{T_{max}} - \beta_2\right) x_{1t}(0)x_{2t}(0) \\ & + (\overline{q}_1^* - 1)\beta_1 x_{1t}(0)x_{3t}(0) - \overline{q}_1^* d_3 x_{2t}(0)x_{4t}(0)\Big\} \\ =& \tilde{\tau}\overline{D}\Big\{ -\frac{r}{T_{max}}\Big[z + \overline{z} + W_{20}^{(1)}(0)\frac{z^2}{2} + W_{11}^{(1)}(0)z\overline{z} + W_{02}^{(1)}(0)\frac{\overline{z}^2}{2} + O(|(z,\overline{z})|^3)\Big]^2 \\ & + \left(\overline{q}_1^*\beta_2 - \frac{\alpha r}{T_{max}} - \beta_2\right)\Big[z + \overline{z} + W_{20}^{(1)}(0)\frac{z^2}{2} + W_{11}^{(1)}(0)z\overline{z} \\ & + W_{02}^{(1)}(0)\frac{\overline{z}^2}{2} + O(|(z,\overline{z})|^3)\Big] \times \Big[q_1 z + \overline{q}_1\overline{z} + W_{20}^{(2)}(0)\frac{z^2}{2} + W_{11}^{(2)}(0)z\overline{z} \end{aligned}$$

$$
\begin{aligned}
&+W_{02}^{(2)}(0)\frac{\overline{z}^2}{2}+O(|(z,\overline{z})|^3)\Big]+(\overline{q}_1^*-1)\beta_1\Big[z+\overline{z}+W_{20}^{(1)}(0)\frac{z^2}{2}\\
&+W_{11}^{(1)}(0)z\overline{z}+W_{02}^{(1)}(0)\frac{\overline{z}^2}{2}+O(|(z,\overline{z})|^3)\Big]\times\Big[q_2z+\overline{q}_2\overline{z}+W_{20}^{(3)}(0)\frac{z^2}{2}\\
&+W_{11}^{(3)}(0)z\overline{z}+W_{02}^{(3)}(0)\frac{\overline{z}^2}{2}+O(|(z,\overline{z})|^3)\Big]-\overline{q}_1^*d_3\Big[q_1z+\overline{q}_1\overline{z}\\
&+W_{20}^{(2)}(0)\frac{z^2}{2}+W_{11}^{(2)}(0)z\overline{z}+W_{02}^{(2)}(0)\frac{\overline{z}^2}{2}+O(|(z,\overline{z})|^3)\Big]\\
&\times\Big[q_3z+\overline{q}_3\overline{z}+W_{20}^{(4)}(0)\frac{z^2}{2}+W_{11}^{(4)}(0)z\overline{z}+W_{02}^{(4)}(0)\frac{\overline{z}^2}{2}+O(|(z,\overline{z})|^3)\Big]\Big\}.
\end{aligned}
$$

The coefficients in (26) are

$$
\begin{aligned}
g_{20}=&2\tilde{\tau}\overline{D}\Big[-\frac{r}{T_{max}}+q_1\Big(\overline{q}_1^*\beta_2-\frac{\alpha r}{T_{max}}-\beta_2\Big)+q_2(\overline{q}_1^*-1)\beta_1-\overline{q}_1^*d_3q_1q_3\Big],\\
g_{11}=&2\tilde{\tau}\overline{D}\Big[-\frac{r}{T_{max}}+\mathrm{Re}\{q_1\}\Big(\overline{q}_1^*\beta_2-\frac{\alpha r}{T_{max}}-\beta_2\Big)+\mathrm{Re}\{q_2\}(\overline{q}_1^*-1)\beta_1\\
&-\overline{q}_1^*d_3\mathrm{Re}\{q_1\overline{q}_3\}\Big],\\
g_{02}=&2\tilde{\tau}\overline{D}\Big[-\frac{r}{T_{max}}+\overline{q}_1\Big(\overline{q}_1^*\beta_2-\frac{\alpha r}{T_{max}}-\beta_2\Big)+\overline{q}_2(\overline{q}_1^*-1)\beta_1-\overline{q}_1^*d_3\overline{q}_1\overline{q}_3\Big],\\
g_{21}=&\tilde{\tau}\overline{D}\Big\{-\frac{r}{T_{max}}\Big(2W_{20}^{(1)}(0)+4W_{11}^{(1)}(0)\Big)+\Big(\overline{q}_1^*\beta_2-\frac{\alpha r}{T_{max}}-\beta_2\Big)\\
&\times\Big(2W_{11}^{(2)}(0)+\overline{q}_1W_{20}^{(1)}(0)+W_{20}^{(2)}(0)+2q_1W_{11}^{(1)}(0)\Big)\\
&+\beta_1(\overline{q}_1^*-1)\Big(2W_{11}^{(3)}(0)+W_{20}^{(3)}(0)+\overline{q}_2W_{20}^{(1)}(0)+2q_2W_{11}^{(1)}(0)\Big)\\
&-\overline{q}_1^*d_3\Big(2q_1W_{11}^{(4)}(0)+\overline{q}_1W_{20}^{(4)}(0)+2q_3W_{11}^{(2)}(0)+\overline{q}_3W_{20}^{(2)}(0)\Big)\Big\}.
\end{aligned}
\tag{28}
$$

From (22) and (24) we have

$$
\begin{aligned}
\dot{W}=&\dot{x_t}-\dot{z}q-\dot{\overline{z}}\overline{q}=\begin{cases}AW-2\mathrm{Re}\{\overline{q}^*(0)f_0q(\theta)\},\ \theta\in[-1,0),\\ AW-2\mathrm{Re}\{\overline{q}^*(0)f_0q(\theta)\}+f_0,\ \theta=0,\end{cases}\\
\triangleq&AW+H(z,\overline{z},\theta),
\end{aligned}
\tag{29}
$$

where

$$
H(z,\overline{z},\theta)=H_{20}(\theta)\frac{z^2}{2}+H_{11}(\theta)z\overline{z}+H_{02}(\theta)\frac{\overline{z}^2}{2}+\cdots. \tag{30}
$$

Substituting the expression into (29) and comparing the coefficients, we have

$$
(A-2i\omega\tilde{\tau})W_{20}(\theta)=-H_{20}(\theta),\ AW_{11}(\theta)=-H_{11}(\theta). \tag{31}
$$

From (29) we know that for $\theta\in[-1,0)$,

$$
H(z,\overline{z},\theta)=-\overline{q}^*(0)f_0q(\theta)-q^*(0)\overline{f}_0\overline{q}(\theta)=-g(z,\overline{z})q(\theta)-\overline{g}(z,\overline{z})\overline{q}(\theta). \tag{32}
$$

From (30) and (32) we have

$$
H_{20}(\theta)=-g_{20}q(\theta)-\overline{g}_{02}\overline{q}(\theta),\ H_{11}(\theta)=-g_{11}q(\theta)-\overline{g}_{11}\overline{q}(\theta). \tag{33}
$$

From (31), (33) and the definition of $A$, we get

$$
\dot{W}_{20}(\theta)=2i\omega\tilde{\tau}W_{20}(\theta)-H_{20}(\theta)=2i\omega\tilde{\tau}W_{20}(\theta)+g_{20}q(\theta)+\overline{g}_{02}\overline{q}(\theta).
$$

For $q(\theta)=(1,q_1,q_2,q_3)^Te^{i\omega\tilde{\tau}\theta}$, we have

$$
W_{20}(\theta)=\frac{ig_{20}}{\omega\tilde{\tau}}q(0)e^{i\omega\tilde{\tau}\theta}+\frac{i\overline{g}_{02}}{3\omega\tilde{\tau}}\overline{q}(0)e^{-i\omega\tilde{\tau}\theta}+E_1e^{2i\omega\tilde{\tau}\theta}, \tag{34}
$$

where $E_1 = (E_1^{(1)}, E_1^{(2)}, E_1^{(3)}, E_1^{(4)})^T \in \mathbb{R}^4$ is a constant vector. Similarly, we obtain

$$W_{11}(\theta) = -\frac{ig_{11}}{\omega\tilde{\tau}} q(0) e^{i\omega\tilde{\tau}\theta} + \frac{i\overline{g}_{11}}{\omega\tilde{\tau}} \bar{q}(0) e^{-i\omega\tilde{\tau}} + E_2, \tag{35}$$

where $E_2 = (E_2^{(1)}, E_2^{(2)}, E_2^{(3)}, E_2^{(4)})^T \in \mathbb{R}^4$ is a constant vector. In what follows, we shall determine the values of $E_1$ and $E_2$. From the definition of $A$ and (31), we have

$$\int_{-1}^{0} d\eta(\theta) W_{20}(\theta) = 2i\omega\tilde{\tau} W_{20}(\theta) - H_{20}(\theta), \quad \int_{-1}^{0} d\eta(\theta) W_{11}(\theta) = -H_{11}(\theta), \tag{36}$$

where $\eta(\theta) = \eta(0, \theta)$. By (29), we have

$$H_{20}(0) = -g_{20} q(0) - \overline{g}_{02} \overline{q}(0) + 2\tilde{\tau} \begin{pmatrix} -\left(\frac{r}{T_{max}} + q_1 \left(\frac{\alpha r}{T_{max}} + \beta_2\right) + \beta_1 q_2\right) \\ q_2\beta_1 + q_1\beta_2 - d_3 q_1 q_3 \\ 0 \\ 0 \end{pmatrix}, \tag{37}$$

and

$$H_{11}(0) = -g_{11} q(0) - \overline{g}_{11} \overline{q}(0) + 2\tilde{\tau} \begin{pmatrix} -\left(\frac{r}{T_{max}} + \mathrm{Re}\{q_1\} \left(\frac{\alpha r}{T_{max}} + \beta_2\right) + \beta_1 \mathrm{Re}\{q_2\}\right) \\ \beta_1 \mathrm{Re}\{q_2\} + \beta_2 \mathrm{Re}\{q_1\} - d_3 \mathrm{Re}\{q_1 \bar{q}_3\} \\ 0 \\ 0 \end{pmatrix}. \tag{38}$$

Substituting the expressions $W_{20}$ and $H_{20}$ into (36), and using following equations

$$\left(i\omega\tilde{\tau} I - \int_{-1}^{0} e^{i\theta\omega\tilde{\tau}} d\eta(\theta)\right) q(0) = 0, \quad \left(-i\omega\tilde{\tau} I - \int_{-1}^{0} e^{-i\omega\tilde{\tau}} d\eta(\theta)\right) \overline{q}(0) = 0,$$

we have

$$\left(2i\omega\tilde{\tau} I - \int_{-1}^{0} e^{2i\theta\omega\tilde{\tau}} d\eta(\theta)\right) E_1 = 2\tilde{\tau} \begin{pmatrix} -\left(\frac{r}{T_{max}} + q_1 \left(\frac{\alpha r}{T_{max}} + \beta_2\right) + \beta_1 q_2\right) \\ q_2\beta_1 + q_1\beta_2 - d_3 q_1 q_3 \\ 0 \\ 0 \end{pmatrix}, \tag{39}$$

which leads to

$$\begin{pmatrix} 2i\omega + \frac{rT_*}{T_{max}} + \frac{s}{T_*} & \frac{\alpha r T_*}{T_{max}} + \beta_2 T_* & \beta_1 T_* & 0 \\ -(\beta_1 V_* + \beta_2 I_*) & 2i\omega + \beta_1 \frac{N d_1}{d_2} T_* & -\beta_1 T_* & d_3 I_* \\ 0 & -\delta & 2i\omega + d_2 & 0 \\ 0 & -pe^{-2i\omega\tilde{\tau}} & 0 & 2i\omega + d_4 \end{pmatrix} E_1$$
$$= 2 \begin{pmatrix} M_1 \\ q_2\beta_1 + q_1\beta_2 - d_3 q_1 q_3 \\ 0 \\ 0 \end{pmatrix}.$$

It follows that

$$E_1^{(1)} = \frac{2}{\Delta_1} \begin{vmatrix} M_1 & \frac{\alpha r T_*}{T_{max}} + \beta_2 T_* & \beta_1 T_* & 0 \\ q_2\beta_1 + q_1\beta_2 - d_3 q_1 q_3 & 2i\omega + \beta_1 \frac{N d_1}{d_2} T_* & -\beta_1 T_* & d_3 I_* \\ 0 & -\delta & 2i\omega + d_2 & 0 \\ 0 & -pe^{-2i\omega\tilde{\tau}} & 0 & 2i\omega + d_4 \end{vmatrix},$$

$$E_1^{(2)} = \frac{2}{\Delta_1} \begin{vmatrix} 2i\omega + \frac{rT_*}{T_{max}} + \frac{s}{T_*} & M_1 & \beta_1 T_* & 0 \\ -(\beta_1 V_* + \beta_2 I_*) & q_2\beta_1 + q_1\beta_2 - d_3 q_1 q_3 & -\beta_1 T_* & d_3 I_* \\ 0 & 0 & 2i\omega + d_2 & 0 \\ 0 & 0 & 0 & 2i\omega + d_4 \end{vmatrix},$$

$$E_1^{(3)} = \frac{2}{\Delta_1}\begin{vmatrix} 2i\omega + \frac{rT_*}{T_{max}} + \frac{s}{T_*} & \frac{\alpha r T_*}{T_{max}} + \beta_2 T_* & M_1 & 0 \\ -(\beta_1 V_* + \beta_2 I_*) & 2i\omega + \beta_1 \frac{Nd_1}{d_2} T_* & q_2\beta_1 + q_1\beta_2 - d_3 q_1 q_3 & d_3 I_* \\ 0 & -\delta & 0 & 0 \\ 0 & -pe^{-2i\omega\tilde{\tau}} & 0 & 2i\omega + d_4 \end{vmatrix},$$

$$E_1^{(4)} = \frac{2}{\Delta_1}\begin{vmatrix} 2i\omega + \frac{rT_*}{T_{max}} + \frac{s}{T_*} & \frac{\alpha r T_*}{T_{max}} + \beta_2 T_* & \beta_1 T_* & M_1 \\ -(\beta_1 V_* + \beta_2 I_*) & 2i\omega + \beta_1 \frac{Nd_1}{d_2} T_* & -\beta_1 T_* & q_2\beta_1 + q_1\beta_2 - d_3 q_1 q_3 \\ 0 & -\delta & 2i\omega + d_2 & 0 \\ 0 & -pe^{-2i\omega\tilde{\tau}} & 0 & 0 \end{vmatrix},$$

where

$$M_1 = -\Big(\frac{r}{T_{max}} + q_1\left(\frac{\alpha r}{T_{max}} + \beta_2\right) + \beta_1 q_2\Big),$$

and

$$\Delta_1 = \begin{vmatrix} 2i\omega + \frac{rT_*}{T_{max}} + \frac{s}{T_*} & \frac{\alpha r T_*}{T_{max}} + \beta_2 T_* & \beta_1 T_* & 0 \\ -(\beta_1 V_* + \beta_2 I_*) & 2i\omega + \beta_1 \frac{Nd_1}{d_2} T_* & -\beta_1 T_* & d_3 I_* \\ 0 & -\delta & 2i\omega + d_2 & 0 \\ 0 & -pe^{-2i\omega\tilde{\tau}} & 0 & 2i\omega + d_4 \end{vmatrix}.$$

Similarly, we have

$$\begin{pmatrix} \frac{rT_*}{T_{max}} + \frac{s}{T_*} & \frac{\alpha r T_*}{T_{max}} + \beta_2 T_* & \beta_1 T_* & 0 \\ -(\beta_1 V_* + \beta_2 I_*) & \beta_1 \frac{Nd_1}{d_2} T_* & -\beta_1 T_* & d_3 I_* \\ 0 & -\delta & d_2 & 0 \\ 0 & -p & 0 & d_4 \end{pmatrix} E_2$$

$$= 2\begin{pmatrix} M_2 \\ \beta_1 \mathrm{Re}\{q_2\} + \beta_2 \mathrm{Re}\{q_1\} - d_3 \mathrm{Re}\{q_1\bar{q}_3\} \\ 0 \\ 0 \end{pmatrix},$$

which leads to

$$E_2^{(1)} = \frac{2}{\Delta_2}\begin{vmatrix} M_2 & \frac{\alpha r T_*}{T_{max}} + \beta_2 T_* & \beta_1 T_* & 0 \\ \beta_1 \mathrm{Re}\{q_2\} + \beta_2 \mathrm{Re}\{q_1\} - d_3 \mathrm{Re}\{q_1\bar{q}_3\} & \beta_1 \frac{Nd_1}{d_2} T_* & -\beta_1 T_* & d_3 I_* \\ 0 & -\delta & d_2 & 0 \\ 0 & -p & 0 & d_4 \end{vmatrix},$$

$$E_2^{(2)} = \frac{2}{\Delta_2}\begin{vmatrix} \frac{rT_*}{T_{max}} + \frac{s}{T_*} & M_2 & \beta_1 T_* & 0 \\ -(\beta_1 V_* + \beta_2 I_*) & \beta_1 \mathrm{Re}\{q_2\} + \beta_2 \mathrm{Re}\{q_1\} - d_3 \mathrm{Re}\{q_1\bar{q}_3\} & -\beta_1 T_* & d_3 I_* \\ 0 & 0 & d_2 & 0 \\ 0 & 0 & 0 & d_4 \end{vmatrix},$$

$$E_2^{(3)} = \frac{2}{\Delta_2}\begin{vmatrix} \frac{rT_*}{T_{max}} + \frac{s}{T_*} & \frac{\alpha r T_*}{T_{max}} + \beta_2 T_* & M_2 & 0 \\ -(\beta_1 V_* + \beta_2 I_*) & \beta_1 \frac{Nd_1}{d_2} T_* & \beta_1 \mathrm{Re}\{q_2\} + \beta_2 \mathrm{Re}\{q_1\} - d_3 \mathrm{Re}\{q_1\bar{q}_3\} & d_3 I_* \\ 0 & -\delta & 0 & 0 \\ 0 & -p & 0 & d_4 \end{vmatrix},$$

$$E_2^{(4)} = \frac{2}{\Delta_2}\begin{vmatrix} \frac{rT_*}{T_{max}} + \frac{s}{T_*} & \frac{\alpha r T_*}{T_{max}} + \beta_2 T_* & \beta_1 T_* & M_2 \\ -(\beta_1 V_* + \beta_2 I_*) & \beta_1 \frac{Nd_1}{d_2} T_* & -\beta_1 T_* & \beta_1 \mathrm{Re}\{q_2\} + \beta_2 \mathrm{Re}\{q_1\} - d_3 \mathrm{Re}\{q_1\bar{q}_3\} \\ 0 & -\delta & d_2 & 0 \\ 0 & -p & 0 & 0 \end{vmatrix},$$

where

$$M_2 = -\Big(\frac{r}{T_{max}} + \mathrm{Re}\{q_1\}\left(\frac{\alpha r}{T_{max}} + \beta_2\right) + \beta_1 \mathrm{Re}\{q_2\}\Big)$$

$$\Delta_2 = \begin{vmatrix} \frac{rT_*}{T_{max}} + \frac{s}{T_*} & \frac{\alpha r T_*}{T_{max}} + \beta_2 T_* & \beta_1 T_* & 0 \\ -(\beta_1 V_* + \beta_2 I_*) & \beta_1 \frac{N d_1}{d_2} T_* & -\beta_1 T_* & d_3 I_* \\ 0 & -\delta & d_2 & 0 \\ 0 & -p & 0 & d_4 \end{vmatrix}.$$

We can determine $W_{20}(\theta)$ and $W_{11}(\theta)$ from (34) and (35). Furthermore, we can compute $g_{21}$ by (28) and obtain following values:

$$\begin{aligned} c_1(0) &= \frac{i}{2\omega\tilde{\tau}}\left(g_{20}g_{11} - 2|g_{11}|^2 - \frac{|g_{02}|^2}{3}\right) + \frac{g_{21}}{2}, \\ \mu_2 &= -\frac{\mathrm{Re}\{c_1(0)\}}{\mathrm{Re}\{\lambda'(\tilde{\tau})\}}, \\ \overline{\beta}_2 &= 2\mathrm{Re}(c_1(0)), \\ T_2 &= -\frac{\mathrm{Im}(c_1(0)) + \mu_2 \mathrm{Im}(\lambda'(\tilde{\tau}))}{\omega\tilde{\tau}}. \end{aligned}$$

**Acknowledgments.** The authors are grateful to the reviewers for their constructive comments and suggestions.

## REFERENCES

[1] A. S. Perelson and P. W. Nelson, Mathematical analysis of HIV-1 dynamics in vivo, *SIAM Rev.*, **41** (1999), 3–44.
[2] P. De Leenheer and H. L. Smith, Virus dynamics: A global analysis, *SIAM J. Appl. Math.*, **63** (2003), 1313–1327.
[3] M. S. Ciupe, B. L. Bivort, D. M. Bortz and P. W. Nelson, Estimating kinetic parameters from HIV primary infection data through the eyes of three different mathematical models, *Math. Biosci.*, **200** (2006), 1–27.
[4] V. Herz, S. Bonhoeffer and R. Anderson, et al., Viral dynamics in vivo: Limitations on estimations on intracellular delay and virus delay, *Proc. Natl. Acad. Sci.* USA, **93** (1996), 7247–7251.
[5] K. A. Pawelek, S. Liu, F. Pahlevani and L. Rong, A model of HIV-1 infection with two time delays: Mathematical analysis and comparison with patient data, *Math. Biosci.*, **235** (2012), 98–109.
[6] R. V. Culshaw and S. G. Ruan, A delay-differential equation model of HIV infection of $CD4^+$ T-cells, *Math. Biosci.*, **165** (2000), 27–39.
[7] J. Mittler, B. Sulzer, A. Neumann and A. S. Perelson, Influence of delayed virus production on viral dynamics in HIV-1 infected patients, *Math. Biosci.*, **152** (1998), 143–163.
[8] P. W. Nelson, J. Murray and A. S. Perelson, A model of HIV-1 pathogenesis that includes an intracellular delay, *Math. Biosci.*, **163** (2000), 201–215.
[9] M. Y. Li and H. Shu, Global dynamics of an in-host viral model with intracellular delay, *Bull. Math. Biol.*, **72** (2010), 1492–1505.
[10] S. Liu and L. Wang, Global stability of an HIV-1 model with distributed intracellular delays and a combination therapy, *Math. Biosci. Eng.*, **7** (2010), 675–685.
[11] R. V. Culshaw, S. Ruan and G. Webb, A mathematical model of cell-to-cell spread of HIV-1 that includes a time delay, *J. Math. Biol.*, **46** (2003), 425–444.
[12] H. Zhu and X. Zou, Dynamics of a HIV-1 infection model with cell-mediated immume response and intracellular delay, *Discrete Contin. Dyn. Syst. Ser. B*, **12** (2009), 513–526.
[13] H. Y. Zhu, Y. Luo and M. L. Chen, Stability and Hopf bifurcation of a HIV infection model with CTL-response delay, *Comput. Math. Appl.*, **62** (2011), 3091–3102.
[14] Y. Wang, Y. Zhou, J. Wu and J. Heffernan, Oscillatory viral dynamics in a delayed HIV pathogenesis model, *Math. Biosci.*, **219** (2009), 104–112.
[15] M. Y. Li and H. Shu, Multiple stable periodic oscillations in a mathematical model of CTL response to HTLV-I infection, *Bull. Math. Biol.*, **73** (2011), 1774–1793.
[16] H. Song, W. Jiang and S. Liu, Virus dynamics model with intracellular delays and immune response, *Math. Biosci. Eng.*,**12** (2015), 185–208.

[17] M. Sourisseau, N. Sol-Foulon, F. Porrot, F. Blanchet and O. Schwartz, Inefficient human immunodeficiency virus replication in mobile lymphocytes, *J. Virol.*, **81** (2007), 1000–1012.
[18] D. S. Dimitrov, R. L. Willey and H. Sato, et al., Quantitation of human immunodeficiency virus type 1 infection kinetics, *J. Virol.*, **67** (1993), 2182–2190.
[19] H. Sato, J. Orenstein, D. S. Dimitrov and M. A. Martin, Cell-to-cell spread of HIV-1 occurs with minutes and may not involve the participation of virus particles, *Virology*, **186** (1992), 712–724.
[20] S. Gummuluru, C. M. Kinsey and M. Emerman, An in vitro rapid-turnover assay for human immunodeficiency virus type 1 replication selects for cell-to-cell spread of virus, *J. Virol.*, **74** (2000), 10882–10891.
[21] J. Witteveldt, M. J. Evans and J. Bitzegeio, et al., CD81 is dispensable for hepatitis C virus cell-to-cell transmission in hepatoma cells, *J. Gen. Virol.*, **90** (2009), 48–58.
[22] J. Lupberger, J. M. B. Zeisel and F. Xiao et al., EGFR and EphA2 are hepatitis C virus host entry factors and targets for antiviral therapy, *Nat. Med.*, **17** (2011), 589–595.
[23] I. Fofana, F. Xiao and C. Thumann, et al., A novel monoclonal anti-CD81 antibody produced by genetic immunization efficiently inhibits Hepatitis C virus cell-cell transmission, *PloS one.*, **8** (2013), e64221.
[24] S. Imai, J. Nishikawa ang K. Takada, Cell-to-cell contact as an efficient mode of Epstein-Barr virus infection of diverse human epithelial cells, *J. Virol.*, **72** (1998), 4371–4378.
[25] Q. J. Sattentau, The direct passage of animal viruses between cells, *Current opinion in virology*, **1** (2011), 396–402.
[26] S. Benovic, T. Kok, A. Stephenson and J. McInnes, et al., De novo reverse transcription of HTLV-1 following cell-to-cell transmission of infection, *Virology.*, **244** (1998), 294–301.
[27] M. L. Dustin and J. A. Cooper, The immunological synapse and the actin cytoskeleton: Molecular hardware for T cell signaling, *Nat Immunol.*, **1** (2000), 23–29.
[28] N. Martin and Q. Sattentau, Cell-to-cell HIV-1 spread and its implications for immune evasion, *Curr Opin HIV AIDS.*, **4** (2009), 143–149.
[29] Q. Sattentau, Avoiding the void: Cell-to-cell spread of human viruses, *Nat Rev Microbiol*, **6** (2008), 815–826.
[30] G. Carloni, A. Crema and M. B Valli, et al., HCV infection by cell-to-cell transmission: Choice or necessity?, *Current molecular medicine.*, **12** (2012), 83–95.
[31] X. L. Lai and X. F. Zou, Modeling HIV-1 virus dynamics with both virus-to-cell infection and cell-to-cell transmission, *SIAM J. Appl. Math.*, **74** (2014), 898–917.
[32] X. L. Lai and X. F. Zou, Modeling cell-to-cell spread of HIV-1 with logistic target cell growth, *J. Math. Anal. Appl.*, **426** (2015), 563–584.
[33] M. Nowak and C. Bangham, Population dynamics of immune responses to persistent viruses, *Science.*, **272** (1996), 74–79.
[34] K. Wang, W. Wang and X. Liu, Global stability in a viral infection model with lytic and nonlytic immune response, *Comput. Math. Appl.*, **51** (2006), 1593–1610.
[35] J. K. Hale and S. M. Verduyn Lunel, *Introduction to Functional Differential Equations*, Springer-Verlag, 1993.
[36] W. M. Hirsch, H. Hanisch and J. P. Gabril, Differential equation models of some parasitic infections: Methods for the study of asymptotic behavior, *Commun. Pure. Appl. Math.*, **38** (1985), 733–753.
[37] J. Hale and W. Z. Huang, Global geometry of the stable regions for two delay differential equations, *J. Math. Anal. Appl.*, **178** (1993), 344–362.
[38] S. Busenberg and K. L. Cooke, *Vertically Transmitted Diseases: Models and Dynamics*, vol. 23. Biomathematics. New York: Springer, 1993.
[39] X. Li and J. Wei, On the zeros of a fourth degree exponential polynomial with applications to an eural network model with delays, *Chaos Solitions Fractals.*, **26** (2005), 519–526.
[40] J. Hale, *Theory of Function Differential Equations*, Springer, Heidelberg, 1977.
[41] B. D. Hassard, N. D. Kazariniff and Y. H. Wan, *Theory and Application of Hopf Bifurcation*, London math society lecture note series, vol. 41. Cambridge University Press, 1981.

Received April 20, 2015; Accepted October 17, 2015.

*E-mail address*: xujinhu09@163.com
*E-mail address*: zhouyc@mail.xjtu.edu.cn, corresponding author